NUREG/CR-5871
PNL-8064
Vol. 1

Development of Equipment Parameter Tolerances for the Ultrasonic Inspection of Steel Components

Application to Components Up to 3 Inches Thick

Prepared by
E. R. Green, S. R. Doctor, R. L. Hockey, A. A. Diaz

Pacific Northwest Laboratory
Operated by
Battelle Memorial Institute

Prepared for
U.S. Nuclear Regulatory Commission

AVAILABILITY NOTICE

Availability of Reference Materials Cited in NRC Publications

Most documents cited in NRC publications will be available from one of the following sources:

1. The NRC Public Document Room, 2120 L Street, NW., Lower Level, Washington, DC 20555
2. The Superintendent of Documents, U.S. Government Printing Office, P.O. Box 37082, Washington, DC 20013-7082
3. The National Technical Information Service, Springfield, VA 22161

Although the listing that follows represents the majority of documents cited in NRC publications, it is not intended to be exhaustive.

Referenced documents available for inspection and copying for a fee from the NRC Public Document Room include NRC correspondence and internal NRC memoranda; NRC bulletins, circulars, information notices, inspection and investigation notices; licensee event reports; vendor reports and correspondence; Commission papers; and applicant and licensee documents and correspondence.

The following documents in the NUREG series are available for purchase from the GPO Sales Program: formal NRC staff and contractor reports, NRC-sponsored conference proceedings, international agreement reports, grant publications, and NRC booklets and brochures. Also available are regulatory guides, NRC regulations in the *Code of Federal Regulations*, and *Nuclear Regulatory Commission Issuances*.

Documents available from the National Technical Information Service include NUREG-series reports and technical reports prepared by other Federal agencies and reports prepared by the Atomic Energy Commission, forerunner agency to the Nuclear Regulatory Commission.

Documents available from public and special technical libraries include all open literature items, such as books, journal articles, and transactions. *Federal Register* notices, Federal and State legislation, and congressional reports can usually be obtained from these libraries.

Documents such as theses, dissertations, foreign reports and translations, and non-NRC conference proceedings are available for purchase from the organization sponsoring the publication cited.

Single copies of NRC draft reports are available free, to the extent of supply, upon written request to the Office of Administration, Distribution and Mail Services Section, U.S. Nuclear Regulatory Commission, Washington, DC 20555.

Copies of industry codes and standards used in a substantive manner in the NRC regulatory process are maintained at the NRC Library, 7920 Norfolk Avenue, Bethesda, Maryland, for use by the public. Codes and standards are usually copyrighted and may be purchased from the originating organization or, if they are American National Standards, from the American National Standards Institute, 1430 Broadway, New York, NY 10018.

DISCLAIMER NOTICE

NUREG/CR-5871
PNL-8064
Vol. 1

Development of Equipment Parameter Tolerances for the Ultrasonic Inspection of Steel Components

Application to Components Up to 3 Inches Thick

Prepared by
E. R. Green, S. R. Doctor, R. L. Hockey, A. A. Diaz

Pacific Northwest Laboratory
Operated by
Battelle Memorial Institute

Prepared for
U.S. Nuclear Regulatory Commission

NUREG/CR-5871
PNL-8064
Vol. 1
R5

Development of Equipment Parameter Tolerances for the Ultrasonic Inspection of Steel Components

Application to Components Up to 3 Inches Thick

Manuscript Completed: April 1992
Date Published: June 1992

Prepared by
E. R. Green, S. R. Doctor, R. L. Hockey, A. A. Diaz

Pacific Northwest Laboratory
Richland, WA 99352

Prepared for
Division of Engineering
Office of Nuclear Regulatory Research
U.S. Nuclear Regulatory Commission
Washington, DC 20555
NRC FIN B2289

Abstract

This report documents work performed at Pacific Northwest Laboratory on the effect of frequency domain equipment interactions on the reliability of ultrasonic inservice inspection. The primary focus of this work is to provide information to the United States Nuclear Regulatory Commission on the acceptability of equipment parameter tolerances as given in the American Society of Mechanical Engineers (ASME) Boiler and Pressure Vessel Code Section XI Appendix VIII.

Mathematical models were developed for the entire ultrasonic inspection system including sound propagation through the inspection sample. The models were used to determine worst-case inspection scenarios for thin sections (piping), and these worst-case inspection scenarios were then used in sensitivity studies to determine the suitability of equipment parameter tolerances. Ultrasonics literature was reviewed to find worst-case inspection scenarios outside the scope of the model used, but none that were significantly worse were found. Experiments were performed to confirm the important modeling results. Methods for reducing parameter sensitivity such as the use of a phase insensitive receiver were also investigated.

The model predicted that ASME Code tolerances for equipment bandwidth are acceptable, but tolerances for center frequency are too broad to provide reliable inspection of worst-case defects using narrow band systems. Experiments confirmed the basic trends predicted by the model, but the model seems to be conservative in that it shows greater sensitivity than is found empirically.

Contents

Figures

Tables

Executive Summary

The purpose of ultrasonic inservice inspection (UT/ISI) of nuclear reactor piping and pressure vessels is the reliable detection and sizing of material defects. Before defects can be sized they must first be detected. This is typically done by analyzing ultrasonic echo waveforms from material defects. Studies performed at PNL and elsewhere have shown that changing the components of an ultrasonic inspection system can greatly affect echo amplitude from a defect even when conventional calibration procedures are used, thus reducing the reliability of defect detection. To address this problem, the American Society for Mechanical Engineers (ASME) Section XI Code Appendix VIII has provided tolerance levels for some equipment parameters (e.g., center frequency and bandwidth). The purpose of this report is to evaluate the effects of frequency domain equipment interactions for setting tolerances for limiting UT equipment parameter variations. This work will determine the acceptability of equipment parameter tolerance requirements in the ASME Code. The current ASME Code requirements are based on engineering judgement (i.e., reasonable estimates).

This report describes the mathematical models developed at PNL (Mart and Doctor 1987, Green and Mart 1989) to provide an analytical basis for recommending operating tolerances to the ASME code. The results of sensitivity studies (Green 1989) performed to determine the effects of equipment parameter changes are presented, and experimental test results are shown to support the important modeling results.

The concept behind the modeling effort is that the amplitude changes between UT/ISI systems are due to the frequency domain interaction of the UT/ISI system spectrum and the material/defect frequency response. The purpose of the models is to calculate equipment spectra and defect/material frequency responses and combine them in sensitivity studies to determine the effects of equipment parameter changes. Since this approach provides great flexibility in investigating equipment changes, this analysis is more rigorous than would be possible with experimental studies and can be used to conduct a more focused experimental study to validate the analytical results.

The studies presented here deal primarily with the repeatability and thus the reliability of manual pulse-echo inspection (45° and 60° shear wave) of thin sections (i.e., piping with wall thicknesses less than three inches/76 mm); however, many of the concepts are applicable to other inspection configurations.

Summary and Conclusions

The model work was very effective in providing trending data to guide the empirical verification work. This methodology provided a more cost effective means to reach definitive conclusions concerning equipment operating tolerances. The detailed summary and conclusions reached in this study are:

- Model predictions were compared with data from multi-frequency experiments, and the validity of the model for predicting and calculating transfer functions for specular reflection from worst-case defects was established.

- The model was used to calculate postulated worst-case transfer functions for seven different combinations of transducer sizes, pipe wall thicknesses, and defect angles. The transfer functions were identified as worst case, because they displayed distinct minima at the equipment center frequency, and this feature produces sensitivity to changing frequency domain equipment parameters.

- An equipment bandwidth sensitivity study was performed using mathematical models for thin sections (piping) using postulated worst-case transfer functions. *The results indicate that the ASME Code Section XI Appendix VIII bandwidth equipment tolerance of 10% is sufficient to ensure 2 dB signal amplitude repeatability.*

- An equipment center frequency sensitivity study was conducted using mathematical models for thin sections employing several combinations of worst-case defects and equipment bandwidth. *The model results indicate that none of the systems considered would be repeatable to within 2 dB after a center frequency change of 20%. The results suggest that a center frequency tolerance of ±10% is not sufficient for inspection systems with bandwidths less than 150%. A tolerance of ±5% appears appropriate for systems with bandwidths between 100% and 150%. A tolerance of 3.5% is indicated for systems with bandwidths between 20% and 100%. Systems with*

bandwidths less than 20% may be too sensitive to center frequency changes to permit repeatable inspection of worst-case defects.

- An experiment was performed to test the center frequency sensitivity of worst-case defect inspection. The experimental results were in general agreement with the modeling results, bu*t the experimental results do not exhibit as much sensitivity to equipment center frequency changes as the modeling results. The experimental results indicate that a center frequency tolerance of ±5% is required for systems with bandwidths less than 30%, and a tolerance of ±10% is required for systems with bandwidths greater than 30%. A requirement of ±20% is not sufficient to guarantee inspection repeatability to within 2 dB for typical inspection systems.* More work needs to be done to determine if the model is overly conservative in that it shows greater sensitivity than is found empirically.

- Calculations revealed that much of the frequency domain equipment parameter sensitivity was due to phase cancellation along the receiving transducer face. It is suggested that the receiving transducer for dual element search units and tandem configuration search units be made as small as possible to reduce sensitivity to equipment changes.

Acknowledgements

This work is supported by the US Nuclear Regulatory Commission under Contract DE-AC06-76RL0 1830; NRC FIN B2289; Dr. Joseph Muscara NRC program monitor; Dr. Steve Doctor PNL program manager.

The ray tracing model was developed with assistance from Dr. Bruce Thompson, and Dr. Tim Gray of Ames Laboratory/Iowa State University, and Dr. Bryron Newberry of the University of Cincinnati (formerly of Ames Laboratory/Iowa State University).

As part of the PISC III program, Risley and Harwell UKAEA laboratories had developed independent laboratory measurements and some of these data were used for model validation.

There are many people to thank who contributed to this work while at PNL. Mr. F. Larry Becker was the PNL program manager ten years ago, when the initial experimental data demonstrating the lack of UT/ISI repeatability with different UT instruments was taken. This work demonstrated the need for the modeling effort reported here. Gary Mart was the technical task leader for the first two years of the modeling effort. He developed the equipment models and wrote the first version of the ray tracing model computer program as well as making many of the model validation measurements. Dr. Morris Good performed several of the model validation experiments. John Deffenbaugh made some of the equipment center frequency sensitivity measurements. Bob Bowey made measurements during the equipment modeling effort. Tom Taylor provided guidance on ASME Code requirements and calibration requirements. Dr. V. Schmitz's (while on a sabbatical from the Fraunhofer Institut fur Zerstorungsfreie Prufverfahren, Saarbrucken, West Germany) modeling work here at PNL provided a guide for the early ray tracing model. Kay Hass assisted in typing this report.

Previous Reports in Series

Doctor, S. R., M. S. Good, E. R. Green, P. G. Heasler, F. A. Simonen, J. C. Spanner, T. T. Taylor, and T. V. Vo. 1991. *Nondestructive Examination (NDE) Reliability for Inservice Inspection of Light Water Reactors*. NUREG/CR-4469, PNL-5711, Vol. 11. Pacific Northwest Laboratory, Richland, Washington.

Spanner, J. C., S. R. Doctor, T. T. Taylor/PNL and J. Muscara/NRC. 1990. *Qualification Process for Ultrasonic Testing in Nuclear Inservice Inspection Applications*. NUREG/CR-4882, PNL-6179. Pacific Northwest Laboratory, Richland, Washington.

Doctor, S. R., J. D. Deffenbaugh, M. S. Good, E. R. Green, P. G. Heasler, F. A. Simonen, J. C. Spanner, T. T. Taylor, and T. V. Vo. 1990. *Nondestructive Examination (NDE) Reliability for Inservice Inspection of Light Water Reactors*. NUREG/CR-4469, PNL-5711, Vol. 10. Pacific Northwest Laboratory, Richland, Washington.

Doctor, S. R., J. D. Deffenbaugh, M. S. Good, E. R. Green, P. G. Heasler, F. A. Simonen, J. C. Spanner, and T. T. Taylor. 1989. *Nondestructive Examination (NDE) Reliability for Inservice Inspection of Light Water Reactors*. NUREG/CR-4469, PNL-5711, Vol. 9. Pacific Northwest Laboratory, Richland, Washington.

Doctor, S. R., J. D. Deffenbaugh, M. S. Good, E. R. Green, P. G. Heasler, F. A. Simonen, J. C. Spanner, and T. T. Taylor. 1989. *Nondestructive Examination (NDE) Reliability for Inservice Inspection of Light Water Reactors*. NUREG/CR-4469, PNL-5711, Vol. 8. Pacific Northwest Laboratory, Richland, Washington.

Doctor, S. R., J. D. Deffenbaugh, M. S. Good, E. R. Green, P. G. Heasler, F. A. Simonen, J. C. Spanner, and T. T. Taylor. 1988. *Nondestructive Examination (NDE) Reliability for Inservice Inspection of Light Water Reactors*. NUREG/CR-4469, PNL-5711, Vol. 7. Pacific Northwest Laboratory, Richland, Washington.

Doctor, S. R., J. D. Deffenbaugh, M. S. Good, E. R. Green, P. G. Heasler, G. A. Mart, F. A. Simonen, J. C. Spanner, T. T. Taylor, and L. G. Van Fleet. 1987. *Nondestructive Examination (NDE) Reliability for Inservice Inspection of Light Water Reactors*. NUREG/CR-4469, PNL-5711, Vol. 6. Pacific Northwest Laboratory, Richland, Washington.

Doctor, S. R., D. J. Bates, J. D. Deffenbaugh, M. S. Good, P. G. Heasler, G. A. Mart, F. A. Simonen, J. C. Spanner, T. T. Taylor, and L. G. Van Fleet. 1987. *Nondestructive Examination (NDE) Reliability for Inservice Inspection of Light Water Reactors*. NUREG/CR-4469, PNL-5711, Vol. 5. Pacific Northwest Laboratory, Richland, Washington.

Doctor, S. R., D. J. Bates, J. D. Deffenbaugh, M. S. Good, P. G. Heasler, G. A. Mart, F. A. Simonen, J. C. Spanner, A. S. Tabatabai, T. T. Taylor, and L. G. Van Fleet. 1987. *Nondestructive Examination (NDE) Reliability for Inservice Inspection of Light Water Reactors*. NUREG/CR-4469, PNL-5711, Vol. 4. Pacific Northwest Laboratory, Richland, Washington.

Collins, H. D. and R. P. Gribble. 1986. *Siamese Imaging Technique for Quasi-Vertical Type (QVT) Defects in Nuclear Reactor Piping*. NUREG/CR-4472, PNL-5717. Pacific Northwest Laboratory, Richland, Washington.

Doctor, S. R., D. J. Bates, R. L. Bickford, L. A. Charlot, J. D. Deffenbaugh, M. S. Good, P. G. Heasler, G. A. Mart, F. A. Simonen, J. C. Spanner, A. S. Tabatabai, T. T. Taylor, and L. G. Van Fleet. 1986. *Nondestructive Examination (NDE) Reliability for Inservice Inspection of Light Water Reactors*. NUREG/CR-4469, PNL-5711, Vol. 3. Pacific Northwest Laboratory, Richland, Washington.

Doctor, S. R., D. J. Bates, L. A. Charlot, M. S. Good, H. R. Hartzog, P. G. Heasler, G. A. Mart, F. A. Simonen, J. C. Spanner, A. S. Tabatabai, and T. T. Taylor. 1986. *Evaluation and Improvement of NDE Reliability for Inservice Inspection of Light Water Reactors*. NUREG/CR-4469, PNL-5711, Vol. 2. Pacific Northwest Laboratory, Richland, Washington.

Doctor, S. R., D. J. Bates, L. A. Charlot, H. D. Collins, M. S. Good, H. R. Hartzog, P. G. Heasler, G. A. Mart, F. A. Simonen, J. C. Spanner, and T. T. Taylor. 1986. *Integration of Nondestructive Examination (NDE) Reliability and Fracture Mechanics, Semi-Annual Report, April 1984 - September 1984*. NUREG/CR-4469, PNL-5711, Vol. 1. Pacific Northwest Laboratory, Richland, Washington.

Good, M. S. and L. G. Van Fleet. 1986. *Status of Activities for Inspecting Weld Overlaid Pipe Joints*.

NUREG/CR-4484, PNL-5729. Pacific Northwest Laboratory, Richland, Washington.

Heasler, P. G., D. J. Bates, T. T. Taylor, and S. R. Doctor. 1986. *Performance Demonstration Tests for Detection of Intergranular Stress Corrosion Cracking*. NUREG/CR-4464, PNL-5705, Pacific Northwest Laboratory, Richland, Washington.

Simonen, F. A. 1984. *The Impact of Nondestructive Examination Unreliability on Pressure Vessel Fracture Predictions*. NUREG/CR-3743, PNL-5062. Pacific Northwest Laboratory, Richland, Washington.

Simonen, F. A. and H. H. Woo. 1984. *Analyses of the Impact of Inservice Inspection Using Piping Reliability Model*. NUREG/CR-3753, PNL-5070. Pacific Northwest Laboratory, Richland, Washington.

Taylor, T. T. 1984. *An Evaluation of Manual Ultrasonic Inspection of Cast Stainless Steel Piping*. NUREG/CR-3753, PNL-5070. Pacific Northwest Laboratory, Richland, Washington.

Bush, S. H. 1983. *Reliability of Nondestructive Examination, Volumes I, II, and III*. NUREG/CR-3110-1, -2, and -3, PNL-4584. Pacific Northwest Laboratory, Richland, Washington.

Simonen, F. A. and C. W. Goodrich. 1983. *Parametric Calculations of Fatigue Cruck Growth in Piping*. NUREG/CR-3059, PNL-4537. Pacific Northwest Laboratory, Richland, Washington.

Simonen, F. A., M. E. Mayfield, T. P. Forte, and D. Jones. 1983. *Crack Growth Evaluation for Small Cracks in Reactor-Coolant Piping*. NUREG/CR-3176, PNL-4642. Pacific Northwest Laboratory, Richland, Washington.

Taylor, T. T., S. L. Crawford, S. R. Doctor, and G. J. Posakony. 1983. *Detection of Small-Sized Near-Surface Under-Clad Cracks for Reactor Pressure Vessels*. NUREG/CR-2878, PNL-4373. Pacific Northwest Laboratory, Richland, Washington.

Busse, L. J., F. L. Becker, R. E. Bowey, S. R. Doctor, R. P. Gribble, and G. J. Posakony. 1982. *Characterization Methods for Ultrasonic Test Systems*. NUREG/CR-2264, PNL-4215. Pacific Northwest Laboratory, Richland, Washington.

Morris, C. J. and F. L. Becker. 1982. *State-of-Practice Review of Ultrasonic In-service Inspection of Class I System Piping in Commercial Nuclear Power Plants*. NUREG/CR-2468, PNL-4026. Pacific Northwest Laboratory, Richland, Washington.

Becker, F. L., S. R. Doctor, P. G. Heasler, C. J. Morris, S. G. Pitman, G. P. Selby, and F. A. Simonen. 1981. *Integration of NDE Reliability and Fracture Mechanics, Phase I Report*. NUREG/CR-1696-1, PNL-3469. Pacific Northwest Laboratory, Richland, Washington.

Taylor, T. T. and G. P. Selby. 1981. *Evaluation of ASME Section XI Reference Level Sensitivity for Initiation of Ultrasonic Inspection Examination*. NUREG/CR-1957, PNL-3692. Pacific Northwest Laboratory, Richland, Washington.

1.0 Introduction

This report summarizes work performed as part of the interaction matrix subtask of the NRC program entitled "Evaluation and Improvement in the Nondestructive Evaluation (NDE) Reliability for Inservice Inspection (ISI) of Light Water Reactors." The purpose of this subtask is to evaluate the effects of frequency domain equipment interactions for setting tolerances for limiting UT equipment parameter variations. This work will determine the acceptability of equipment requirements in ASME Code Section XI Appendix VIII. The requirements in the Code Appendix are based on engineering judgement (i.e., reasonable estimates). Results of this study are to used to improve the reliability of piping and pressure vessel inspections. Portions of this work have been published elsewhere (Doctor et al. 1986a, Doctor et al. 1986b, Doctor et al. 1986c, Doctor et al. 1987a, Doctor et al. 1987b, Doctor et al. 1988, Doctor et al. 1989, Green and Mart 1989, Mart and Doctor 1987, Green 1989, Green 1990), but this is the first comprehensive report on the work performed on this subtask.

The purpose of ultrasonic in-service inspection (UT/ISI) of nuclear reactor piping and pressure vessels is the reliable detection and sizing of material defects. Before defects can be sized they must first be detected. This is typically done by analyzing ultrasonic echo waveforms with an amplitude greater than a certain percentage of that of a calibration reflector (ASME Section XI, Appendix III) such as a 10% notch, side-drilled hole, or flat-bottomed hole.

Studies performed at PNL (Doctor et al. 1986a, Posakony 1986) and elsewhere (Borloo et al. 1988, MacDonald and Walker 1987, Gregor 1984) have shown that changing the components of an ultrasonic inspection system can greatly affect echo amplitude from a defect even when conventional calibration procedures (ASME Section XI, Appendix III) are used, thus reducing the reliability of defect detection. To address this problem, ASME Code Section XI Appendix VIII has provided tolerance levels for some equipment parameters (e.g., center frequency and bandwidth). However, these code requirements are based on engineering judgement and lack a strong analytical foundation.

This report describes the mathematical models developed at PNL (Mart and Doctor 1987, Green and Mart 1989) to provide an analytical basis for developing improved recommendations for the ASME code. The results of sensitivity studies (Green 1989) performed to determine the effects of equipment parameter changes are presented, and experimental test results are shown to support the important modeling results.

The concept behind the modeling effort is that amplitude changes between UT/ISI systems are due to the frequency domain interaction of the UT/ISI system spectrum and the material/defect frequency response. The purpose of the models is to calculate equipment spectra and defect/material frequency responses and combine them in sensitivity studies to determine the effects of equipment parameter changes. Since this approach provides great flexibility in investigating equipment changes, this analysis is more rigorous than would be possible with experimental studies and can be used to conduct a more focused experimental study to validate the model predictions.

The studies presented here deal primarily with the repeatability and thus the reliability of manual pulse-echo inspection (45° and 60° shear wave) of thin sections (piping with wall thicknesses less than three inches/76 mm), however, many of the concepts are applicable to other inspection configurations.

Section 2 describes the equipment models that were developed, while Section 3 describes the defect model that models the propagation of the elastic sound field from the transducer through all the intervening layers to the defect and back to the receiving transducer. Section 4 provides the fundamental concept for determining worst-case changes that can occur in ultrasonic signal amplitude that result from interactions between the defect and the equipment. The worst-case defects are defined in this section for the various equipment and inspection conditions considered in this study. Section 5 provides the details of the sensitivity studies that were conducted for all parameters studied. Section 6 delineates the summary and conclusions that can be derived from this work, and Section 7 identifies the future direction of this work.

2.0 Equipment Models

A generic ultrasonic inspection system is shown in Figure 2.1, and Figure 2.2 is the corresponding block diagram. Several difficulties are encountered in modeling this system. The pulser output waveform differs depending upon the impedance of the cable and transducer. The transducer input impedance, though nominally rated as 50 ohms, can vary with frequency from a few ohms to thousands of ohms, and the impedance plots for different transducers can also vary greatly in shape depending on transducer construction and the tuning circuit employed.

Modeling of the transducer and pulser (Mart and Doctor 1987) was approached in two different ways. The first approach was to model the pulser using a commercially available circuit analysis program and to model the transducer using the KLM model (Silk 1984). This approach was abandoned because the circuit analysis program required discrete circuit components, and the KLM model output was a plot of the transducer input impedance as a function of frequency. Also, the circuit analysis program was not able to accurately model the key semiconductor components of the pulser because they behaved nonlinearly. The second approach was to accurately measure the transducer transfer function (ratio of the sound pressure produced to the applied voltage as a function of frequency) and assume that the input impedance of the transducer was large in relation to the pulser output impedance. In effect, it was assumed that the transducer input impedance would not affect significantly the output of the pulser. This assumption was not good, but no satisfactory modeling alternative existed. The modeling work for the pulser and transducer was never satisfactorily completed.

The receiver is a relatively simple instrument consisting of attenuators, amplifiers, and simple filters. A well designed instrument would have an input impedance of 50 ohm over the measurement frequency range; however, a wide range of values was observed between receivers and on the same receiver as front-panel controls were adjusted (Doctor and Mart 1987). The receiver was "modeled" in terms of measured input impedance and gain as a function of frequency (i.e., the receiver was replaced by its Thevenin equivalent).

Faced with the difficulties of modeling the individual components, a simpler approach is used in the work reported here. The electrical equipment is modeled as a waveform that represents the response of the inspection system for an acoustic system frequency response of unity amplitude and zero phase. The waveform represents the combined response of the pulser, cables, piezoelectric transducers, receiver, and video display. The Fast Fourier Transform (FFT) of the waveform is taken to determine the equipment spectrum. The equipment spectrum is multiplied by the acoustic system frequency response as calculated by the defect model (both are complex) to obtain a response spectrum which is inverse FFT'ed to yield the inspection system echo response (A-scan) for a given defect.

The representative waveform approach allows the difficulties of modeling to be avoided. The issue of the interaction of the pulser and the transducer is avoided by considering them as a single system which provides sound input to the acoustic portion of the inspection system. In other words, the pulser and transducer combined are a type of black box that produces motion at the transmitting transducer face. In much the same way, the receiving transducer and the receiver are combined as a black box that produces voltage depending on the motion at the receiving transducer face. To apply linear control theory concepts it is necessary to assume that the receiving black box and the acoustical system are linear systems. This is a reasonable assumption for normal ultrasonic inspection as long as the receiver is being operated properly. It is not necessary to assume that the transmitting black box is linear as it only provides input to the other systems. The acoustical system includes the effects of the transmitting and receiving transducer directivity patterns, time-of-flight delays, beam spread, material attenuation, and flaw scattering. The waveform (A-scan) produced by the ultrasonic inspection system is:

$$s(t) = p(t) * h_1(t) * h_2(t) \qquad (1)$$

where p(t) is the transducer surface displacement produced by the transmitting black box, $h_1(t)$ is impulse response (response to a hypothetical unit impulse) of the acoustic system, $h_2(t)$ is the impulse response of the receiving black box, and * is the convolution operator. In the frequency domain:

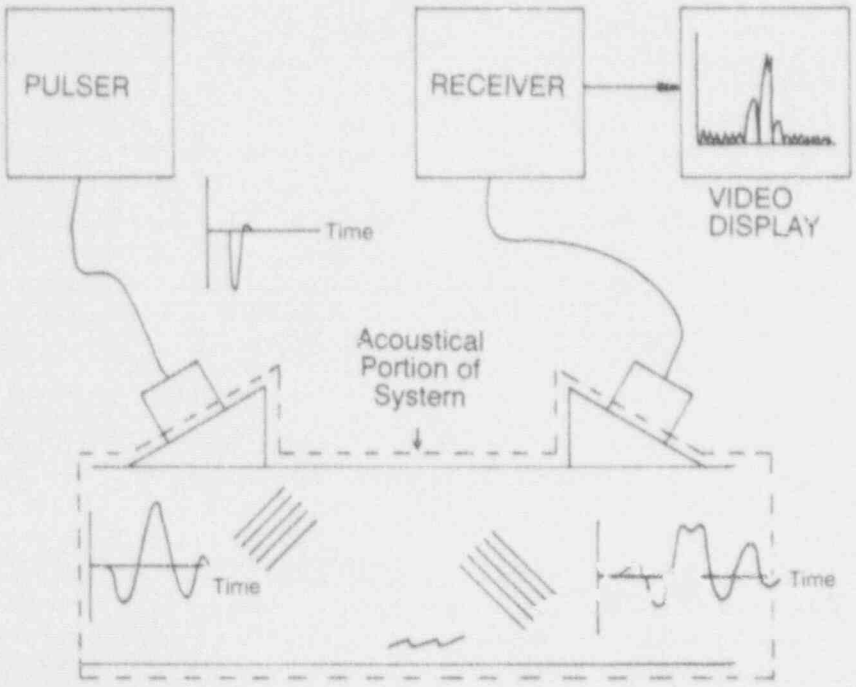

Figure 2.1. Generic Ultrasonic Inspection System

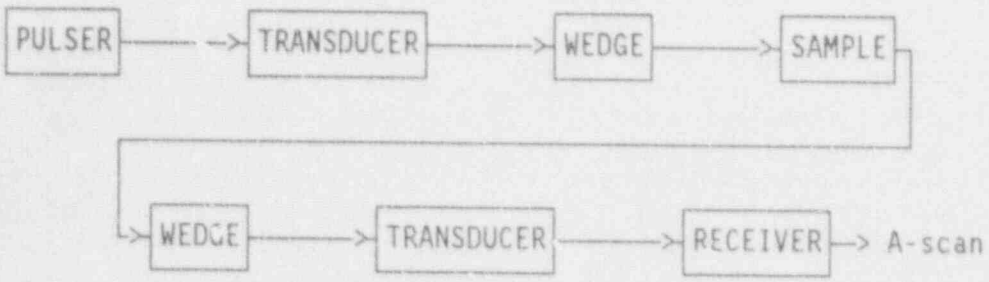

Figure 2.2. Block Diagram of Ultrasonic Inspection Systems

$$S(w) = P(w)H_1(w)H_2(w) \quad (2)$$

where S, P, H_1, and H_2 are the frequency domain representations of s, p, h_1, and h_2, respectively. The angular frequency is w.

Now, the response can be rearranged as:

$$S(w) = P(w)H_2(w)H_1(w) \quad (3)$$

or

$$S(w) = H_3(w)H_1(w) \quad (4)$$

where H_3 is the product of P and H_2. Note that H_3 is the equipment spectra of the system. The A-scan waveform can now be written as:

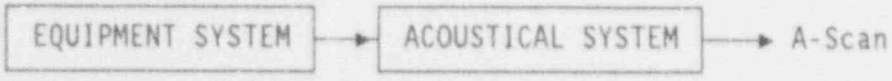

Figure 2.3. Block Diagram of Condensed Ultrasonic Inspection System

$$s(t) = h_3 * h_1 \qquad (5)$$

as represented in the block diagram in Figure 2.3. The term h_3 is a waveform representative of the equipment system (ie., the waveform that would be obtained if the acoustic system had unity gain at all frequencies).

The use of a representative waveform provides tremendous flexibility, because the analysis can use either measured waveforms obtained using an ultrasonic reflector with an approximately flat spectral reflectance over the frequency range of interest or hypothetical waveforms of any type. For the studies presented here, a cosine-squared-windowed sine wave with the window centered on a positive going peak was used. The center frequency is the frequency of the sine wave, and the bandwidth depends upon the length of the windowing function. The cosine-squared-windowed sine wave closely approximates the waveforms of many inspection systems both narrow and broadband. The spectrum of the cosine-squared-windowed sine wave is a bell shaped curve.

To limit the scope of the work presented here, the effect of varying equipment bandwidth and center frequency using similarly shaped equipment waveforms was investigated. This approach presupposes that the waveforms from different ultrasonic inspection instruments are similar. This is not the case, but measuring the effect of varying all possible ultrasonic test system variables (pulse rise time, pulse fall time, pulse shape, cable construction, transducer impedance, transducer construction, etc.) would require a program of much larger scope. The representative waveform approach using equipment model results could be used for this expanded analysis. The waveforms from different ultrasonic inspection instruments are believed to be similar enough that the approach used here which models changes in the amplitude of the equipment spectrum will indicate primary effects while parameter changes that affect the phase of the equipment spectrum will produce only secondary effects. The actual effects of changes in the phase of the equipment spectrum is an area where further research could be performed.

3.0 Defect Model

3.1 Model Theory

A two-dimensional, ray tracing model to calculate the acoustic system transfer function (H_1 of Section 2) of a steel sample with a surface-connected crack is described. The model can simulate either a pitch-catch/tandem arrangement as shown in Figure 2.1 or a pulse-echo arrangement. The crack simulation model calculated frequency responses are used in conjunction with frequency spectra representative of the electronics of a UT/ISI system (H_3 of Section 2) to investigate frequency domain equipment interactions. The model considers only specular reflection from the crack. Crack tip diffraction and diffuse scattering are not considered.

The crack simulation model is based on ray tracing methods similar to those used by Scruby, et al (1986) except that crack tip diffraction is not included. Other methods besides ray tracing exist for the modeling of wave propagation in solids including finite element analysis, finite difference analysis, modal analysis (T-matrix), and solution of the governing integral equations (Langenberg and Schmitz 1986, Temple 1985, Bond 1982). The ray tracing method was chosen for the model used here, because the calculation time is relatively short which is required, since calculations are completed for many frequencies.

The model program consists of approximately 40 pages (including comment statements) of FORTRAN 77 code. To date, the program has only been run on a DEC VAX 11/780 computer. A typical run time is 30 minutes with no other computer users; though, the run time can vary from several minutes to several hours depending on the application.

The flow chart for the model computer program is shown in Figure 3.1. First, the analyst selects the path of interest (e.g., a shear wave reflecting from the crack as a shear wave, or a longitudinal wave reflecting from the sample bottom as a longitudinal wave, etc.). This is done so that only similar incident wave fronts are integrated at the receiving transducer face as explained below.

The face of the sending transducer is divided into elements that are small with respect to the wavelength. The center of each element is a site from which the rays originate. The original phase and amplitude of a ray is calculated using the appropriate directivity functions (Miller and Pursey 1953, Equations 93 and 94). The directivity functions are the shear and longitudinal velocity fields in a semi-infinite solid caused by an infinitely long strip of constant amplitude, sinusoidally varying pressure acting normal to the free surface. As the width of the strip is made much smaller than the wavelengths of sound produced, the directivity functions describe the behavior of a fluid pressure line source. The directivity functions for shear and longitudinal waves in acrylic plastic (c_L = 2.73 mm/us and c_T = 1.43 mm/us) are shown in Figures 3.2 through 3.5. The corresponding equations for shear and longitudinal waves are given below in Eqns. (6) and (7), respectively. Note that "^" indicates a complex variable (i.e., one having amplitude and phase). The directivity functions are valid in the far-field region of the transducer element. As the size of the transducer elements becomes small, their near field likewise becomes small, and the model can predict both near and far field of the assemblage of transducer elements. In the model, both the amplitude and phase of the directivity expressions are used. Only the longitudinal Miller and Pursey directivity pattern is used typically, since the production of transverse waves by a longitudinal mode transducer is known to be insignificant for the configurations considered.

$$\hat{D}_T(\theta) = \frac{j\mu^{2.5}\sin 2\theta\sqrt{\mu^2\sin^2\theta - 1}}{(2\mu^2\sin^2\theta - \mu^2)^2 - 4\mu^2\sin^2\theta\sqrt{\mu^2\sin^2\theta - 1}\sqrt{\mu^2\sin^2\theta - \mu^2}} \tag{6}$$

$$\hat{D}_L(\theta) = \frac{\cos\theta\,(\mu^2 - 2\sin^2\theta)}{(2\sin^2\theta - \mu^2)^2 - 4\sin^2\theta\sqrt{\sin^2\theta - 1}\sqrt{\sin^2\theta - \mu^2}} \tag{7}$$

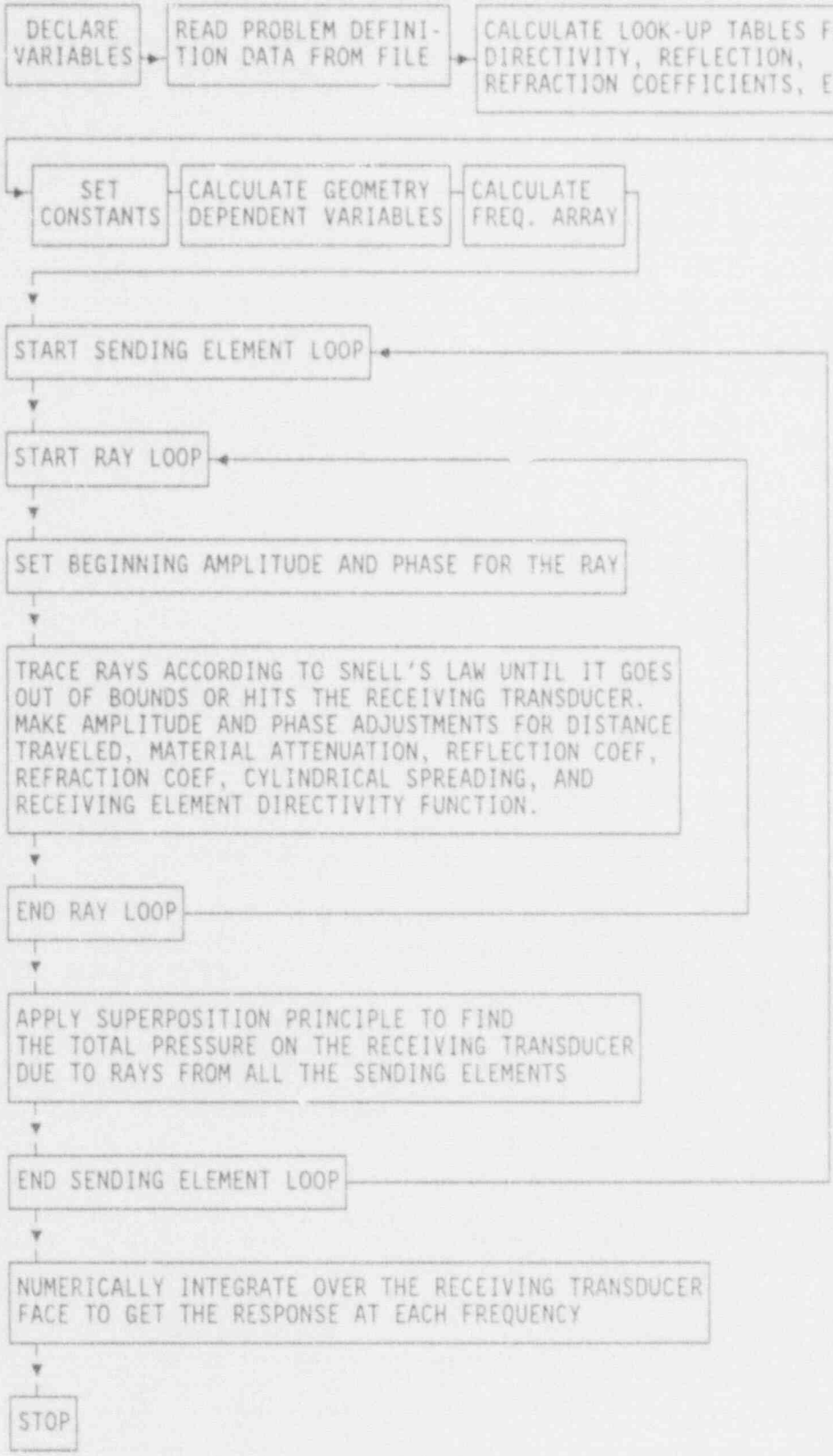

Figure 3.1. Flow Chart for the Model Computer Program

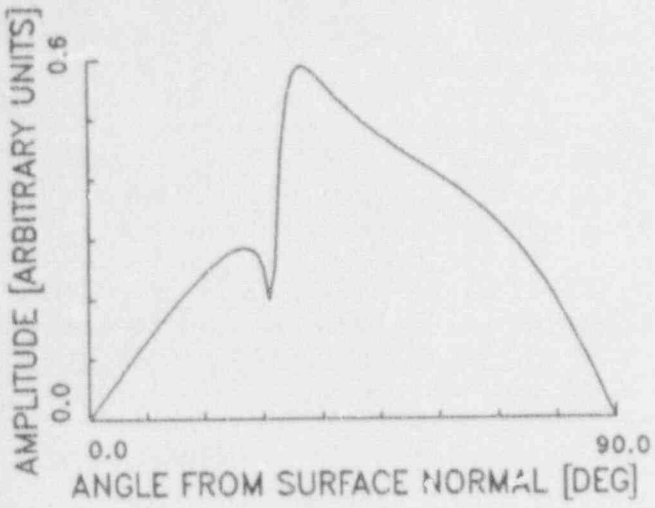

Figure 3.2. Amplitude of the Directivity Function for the Line Source Generation of Transverse Waves in Acrylic Plastic

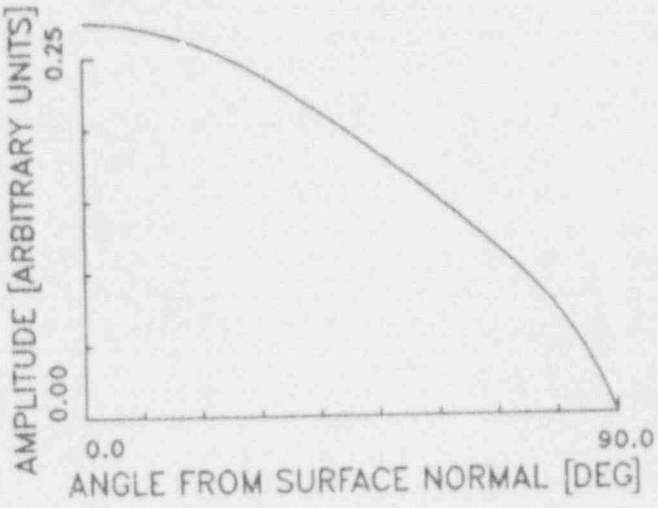

Figure 3.4. Amplitude of the Directivity Function for the Line Source Generation of Longitudinal Waves in Acrylic Plastic

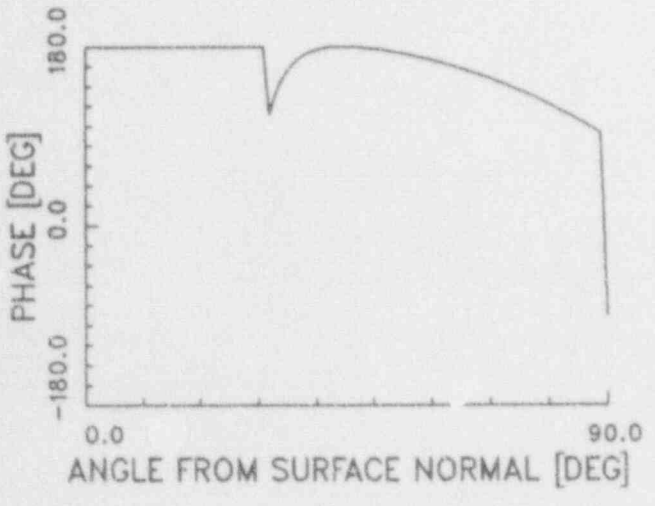

Figure 3.3. Phase of the Directivity Function for the Line Source Generation of Transverse Waves in Acrylic Plastic

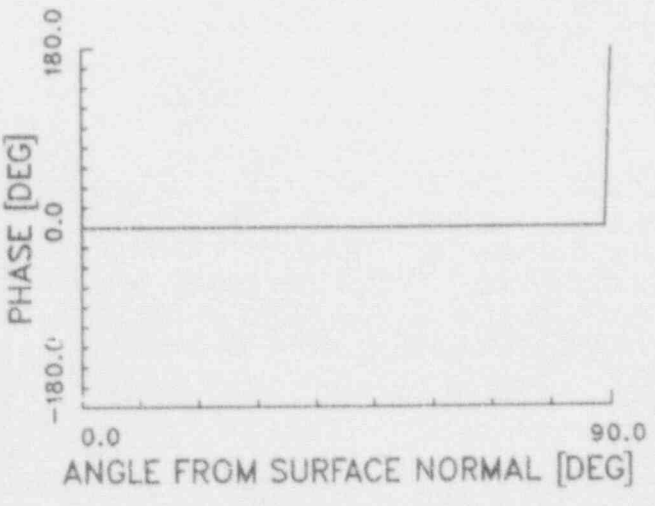

Figure 3.5. Phase of the Directivity Function for the Line Source Generation of Longitudinal Waves in Acrylic Plastic

where θ is the angle measured from surface normal, $a = c_L/c_T$, c_L is the longitudinal wave speed, c_T is the transverse wave speed, and j is the square root of -1.

If in future work it is necessary to reduce computation time, the possibility of assuming a perfectly cylindrical source directivity function could be investigated. This may work well, since all of the rays that eventually intersect the receiving transducer leave the sending transducer element at approximately the same angle, and the Miller and Pursey longitudinal directivity function varies slowly for angles near surface normal.

After leaving the source element, a ray is traced until it either goes out of bounds or intersects the receiving transducer face. The material medium is assumed to be isotropic and homogenous. Within a medium (acrylic wedge or steel sample), a ray travels in a straight line and is attenuated based on the change in the radius of curvature per Eqn. (8), where cylindrical spreading consistent with the 2-D model has been assumed. Usually in a ray tracing program, the amplitude is calculated based on the spacing between the rays rather than keeping track of the wavefront's radius of curvature. The approach taken here requires fewer rays, and, therefore, requires less computation time, but requires that the wavefront be assumed to be roughly circular. Attenuation by a factor of 1/r as for a spherical wavefront (3-D far field) was found to produce only slightly different results in the calculated acoustic system transfer function. The ray's phase is decreased according to the number of wavelengths traveled. Within the wedge, a ray's amplitude is also decreased exponentially with respect to distance traveled to account for material attenuation per Eqn. (9).

$$A_{NEW} = A_{OLD}\sqrt{\frac{R_{OLD}}{R_{NEW}}} \tag{8}$$

$$A_{NEW} = A_{OLD}\, e^{-\alpha d} \tag{9}$$

where A is the ray amplitude, R is the radius of curvature of the wavefront, α is the material attenuation in nepers/mm, and d is the distance traveled between the old and new positions in millimeters.

When a ray leaves the sending wedge or enters the receiving wedge through the couplant, the amplitude and phase of the transmitted ray that follows the path of interest are calculated using the transmission coefficients of Kuhn and Lutsch (1961, from Eqns 3c and 3d) per Eqns (10), (11), (12), and (13). Krautkramer and Krautkramer (1983, pp. 607-617) give an alternate form of these equations that does not include phase. The transmission coefficients are modified slightly to make them ratios of velocity amplitude rather than velocity potential amplitude. The radius of curvature is also changed in accordance with the change in the speed of a ray as it goes from one material to another per Eqn. (14). The assumption is made that the cylindrical wavefront (2-D far field) remains cylindrical after refraction from one material to the next.

$$\hat{T}_{LL} = \frac{c'^2_T}{c^2_T}\,\frac{(b^2-1)(b'^2-1)}{a'(\Delta+k\Delta')} \tag{10}$$

$$\hat{T}_{LT} = \frac{c_L}{c_T}\,\frac{c'^4_T}{c^2_T}\,\frac{2(b^2-1)}{(\Delta+k\Delta')} \tag{11}$$

$$\hat{T}_{TL} = \frac{c_L}{c_T}\,\frac{c'^2_T}{c^2_T}\,\frac{2b(b'^2-1)}{a'(\Delta+k\Delta')} \tag{12}$$

$$\hat{T}_{TT} = \frac{c'^2_T}{c^2_T}\,\frac{4b}{(\Delta+k\Delta')} \tag{13}$$

$$R_{NEW} = R_{OLD}\sqrt{\frac{c_{OLD}}{c_{NEW}}} \tag{14}$$

where $\Delta=[(b^2-1)^2/2a]+2b$, $\Delta'=[(b'^2-1)^2/2a']+2b'$, $k=\rho' c'^4_T/\rho c^4_T$, $a=[(c^2/c^2_L)-1]^{.5}$, $a'=[(c^2/c'^2_L)-1]^{.5}$, $b=[(c^2/c^2_T)-1]^{.5}$, $b'=[(c^2/c'^2_T)-1]^{.5}$, $c=c_L/\sin(\alpha_T)$, α_L is the angle measured from surface normal for the incident longitudinal wave, "'" indicates properties for the second medium, and the TL subscript indicates transmission of a transverse wave to a longitudinal

wave, etc. Also, R_{NEW}, R_{OLD}, c_{OLD}, c_{NEW} are the new and old radii of curvature and wavefront speeds.

When a ray reflects from a boundary, the amplitude and phase of the reflected ray that follows the path of interest are calculated using the reflection coefficients per Krautkramer and Krautkramer (1983, p.605) and also Graff (1975, pp. 317-322) as in Eqns. (15), (16), (17), and (18). Like the transmission coefficients, the reflection coefficients are modified slightly to make them ratios of velocity amplitude rather than velocity potential amplitude. It is assumed that the boundary (bottom surface, defect, etc.) is a free boundary (i.e., no stresses). The radius of curvature is changed if a mode conversion occurs (i.e., the ray speed changes) per Eqn. (14). It is assumed that the cylindrical wavefront remains cylindrical after reflection from a planar surface both with and without mode conversion.

$$\hat{R}_{LL} = \frac{\mu^{-2}\sin 2\alpha_L \sin 2\alpha_T - \cos^2 2\alpha_T}{\mu^{-2}\sin 2\alpha_L \sin 2\alpha_T + \cos^2 2\alpha_T} \tag{15}$$

$$\hat{R}_{LT} = \frac{-2\mu^{-1}\sin 2\alpha_L \cos 2\alpha_L}{\mu^{-2}\sin 2\alpha_L \sin 2\alpha_T + \cos 2\alpha_T} \tag{16}$$

$$\hat{R}_{TL} = \frac{\mu^{-1}\sin 4\alpha_T}{\mu^{-2}\sin 2\alpha_L \sin 2\alpha_T + \cos^2 2\alpha_T} \tag{17}$$

$$for\ \alpha_T < \alpha_{crit}$$

$$\hat{R}_{TL} = 0 \tag{18}$$

$$for\ \alpha_T \geq \alpha_{crit}$$

$$\hat{R}_{TT} = \hat{R}_{LL} \tag{19}$$

$$for\ \alpha_T < \alpha_{crit}$$

$$\hat{R}_{TT} = -1 + 0j \tag{20}$$

$$for\ \alpha_T \geq \alpha_{crit}$$

where α_T and α_L are the angles measured from surface normal for the transverse and longitudinal waves, respectively, $\mu = c_L/c_T$, $\alpha_{crit} = \mathrm{Sin}^{-1}(c_T/c_L)$ is the critical angle ,and the TL subscript indicates reflection of a transverse wave to a longitudinal wave, etc.

The final amplitude and phase of a ray that intersects the receiving transducer face is calculated based on the incident values and the appropriate Miller and Pursey directivity functions (Eqns. 6 and 7). It is assumed by reciprocity that the Miller and Pursey directivity functions are valid for receiving elements, as they are for sending elements. The amplitude, phase, and intersection position of each ray intersecting the receiving transducer is recorded. To obtain the pressure incident on the receiving transducer face due to a single sending transducer element, the recorded intersection information for the element is examined. In order to determine the incident pressure at regular spacings along the receiving transducer face, values are determined by linear interpolation of the irregularly spaced recorded data. Here it is required that the angular spacing between the rays be close enough to allow accurate linear interpolation. Because all of the recorded data are from the same path of interest (the path of interest is selected by the analyst at the beginning of the modeling calculation), a smooth curve is formed when plotted against position, and linear interpolation is possible.

To determine the incident pressure at a point on the receiving transducer face due to the entire sending transducer, the interpolated pressures at the point for each sending transducer element are added vectorially. The receiving transducer has only a single output voltage port, and the output voltage at this port is taken to be proportional to the integrated pressure over the transducer face. Thus, the receiving transducer face is assumed to be locally reactive (Chapman 1984). The integration is performed numerically using the trapezoidal rule, and both the amplitude and phase of the pressure are used.

By repeating the above single frequency calculations for a range of frequencies, the frequency response of the path of interest is calculated. The frequency response

of the entire acoustical system is calculated by adding vectorially the frequency responses of the significant paths of interest.

3.2 Model Assumptions and Limitations

Several assumptions are made in the sample model:

1. Diffraction effects are ignored (i.e., only specular reflection from the defect is considered). The specular reflection assumption is valid for specular reflection from defects larger than approximately three wavelengths. The specular reflection assumption is especially good for specular reflection from smooth defects that are larger than the ultrasonic beam width. The specular reflection assumption is an important limitation, because diffraction scattering can be important in the detection and sizing of small defects, rough defects such as intergranular stress corrosion cracks, and large smooth cracks at nonspecular angles. In defense of the model, it predicts the behavior of large cracks which are generally a greater structural integrity concern than small cracks. False calls of small cracks tend to be more a financial concern rather than a structural integrity concern. A more extensive discussion of the weaknesses of the elastodynamic Kirchhoff theory (which is similar to the theory used in this model except that it weakly estimates diffraction effects) is given by Chapman (1984).

2. The model is two-dimensional. To reduce computation time, the propagation of sound through three-dimensional media is modeled in two dimensions. Errors associated with this assumption do not seem to be great for defects longer than the beam width as evidenced by the results presented in the model validation section. However, the model does not account for defect skew (only defect tilt), and this is a limitation; however, weld cracks are typically either circumferentially or longitudinally oriented. Furthermore, since the model is trying to determine worst-case defects, the changes resulting from skew should not produce equipment interaction results worse than those resulting from tilt.

3. The defect is assumed to be flat, smooth, traction free, and the two sides of the defect are assumed not to be in contact. A discussion of assumptions relating to the defect is given by Chapman (1984).

4. The acoustic system is assumed linear and invariant so that the principle of superposition and transfer function theory (Goodman 1968) can be applied. This is a reasonable first assumption for UT/ISI.

5. The receiving transducer is assumed to be locally reactive. The effect of this assumption is not believed to be large for typical UT transducers. This assumption would tend to overestimate the degree of constructive and destructive interference possible at the transducer face, thus, making the acoustic system transfer function slopes greater than those possible in real systems. The result is an exaggeration of the effects of equipment parameter changes making the model conservative in this respect.

6. At this stage of development, the model can only consider reflection from planar boundaries. This prevents the modeling of reactor nozzles. Future work will include modifying the model to include curved boundaries.

7. It is assumed that the cylindrical wavefront remains cylindrical after refraction from one material to the next and after reflection with mode conversion. Geometrical constructions show that this assumption is reasonable except when the angle from surface normal is highly oblique. This limits the model to inspection angles of 60° SV or less.

3.3 Model Validation

As a first step in validating the ray tracing model, single frequency sound field measurements were made along the bottom centerline of an acrylic wedge as shown in Figure 3.6 and compared against model predictions. A tone burst was used as input to the transducer. A 1.0-inch (25-mm) diameter transmitting transducer was used for the 500-kHz and 1-MHz experiments, and a 1/4-inch (6-mm) diameter transmitting transducer was used at 2 MHz and 5 MHz. The pressure field along the wedge bottom was measured using a PNL

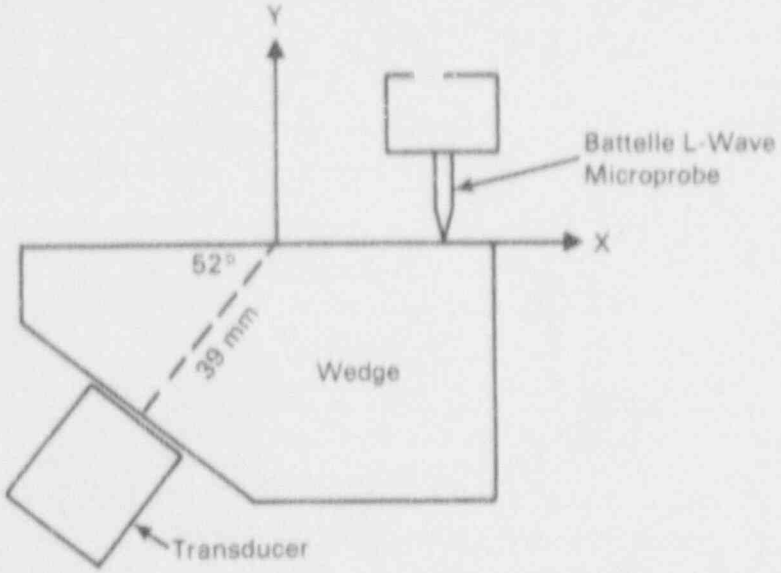

Figure 3.6. Configuration for Measuring the Single Frequency Ultrasonic Sound Field along the Centerline of an Acrylic Wedge

constructed longitudinal wave microprobe consisting of a 0.010-inch (0.25-mm) diameter piezoelectric elemen.

The results at 500 kHz, 1 MHz, 2 MHz, and 5 MHz are shown in Figures 3.7 through 3.10, respectively. These results were normalized to a peak value of 1.0. Agreement between the experimental and calculated sound fields is good at all frequencies. The results are good considering the fact that the circular-faced transducers are modeled in two dimensions as long strips.

In the second test of the model's validity, model predictions were compared with results from a number of single-frequency experiments. The first experiment was a 90° corner reflection measurement at 5 MHz. Figure 3.11 shows the variation in signal amplitude of a 45° SV, pulse-echo probe as a function of distance from a 90° corner in a 20.8-mm-thick steel block. The corner reflection signal was made up of ultrasound from two different paths within the block -- the transducer/end/bottom/transducer and transducer/bottom/end/transducer paths. Agreement between the model prediction and experimental measurement was excellent. The excellent agreement was especially significant, since it showed that under certain conditions a two-dimensional model can be used to model more complex three-dimensional inspection configurations such as this measurement in which a circular transducer was used.

In the next set of single-frequency, validation experiments, the centerline beam patterns of 45° longitudinal and 45° SV transmission through a 133-mm-thick steel block were measured at 1 MHz. An immersion setup was used with a non-focused probe for excitation and PNL L-wave and S-wave microprobes (Good and Green 1989) for L-wave and S-wave reception, respectively. The comparisons between model predictions and experimental measurements for the two cases are shown in Figures 3.12 and 3.13. The comparison for 45° L-wave transmission was excellent for both the main lobe (centered at 110 mm) and the secondary lobe (centered at 16 mm). The comparison for 45° SV-wave transmission was good but not excellent. It was believed that differences between model and experiment results were due to measurement errors related to the directivity pattern of the S-wave microprobe.

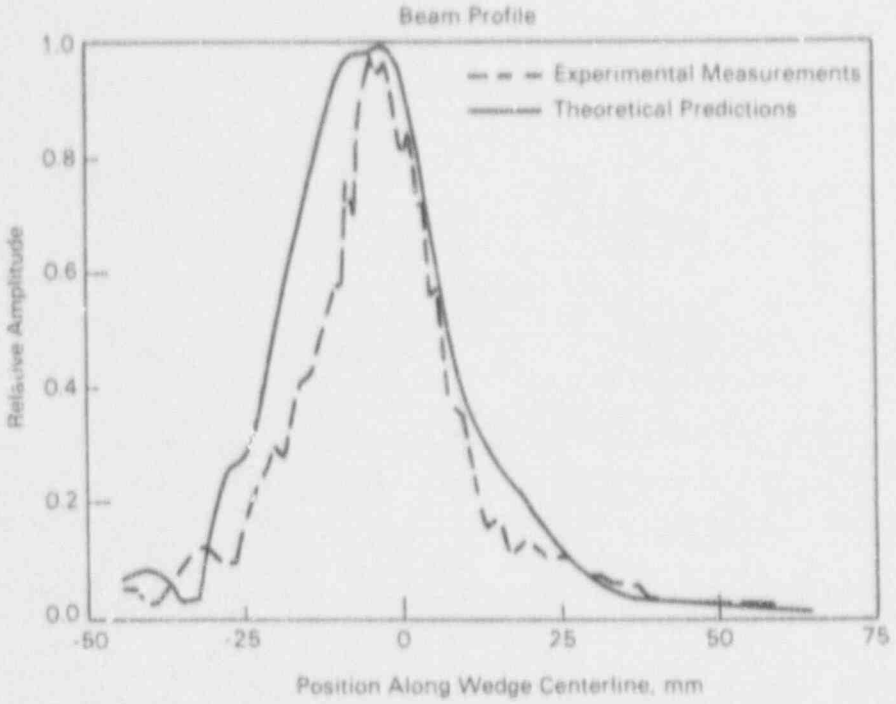

Figure 3.7. Predicted Versus Measured Sound Field along the Wedge Centerline at 500 kHz

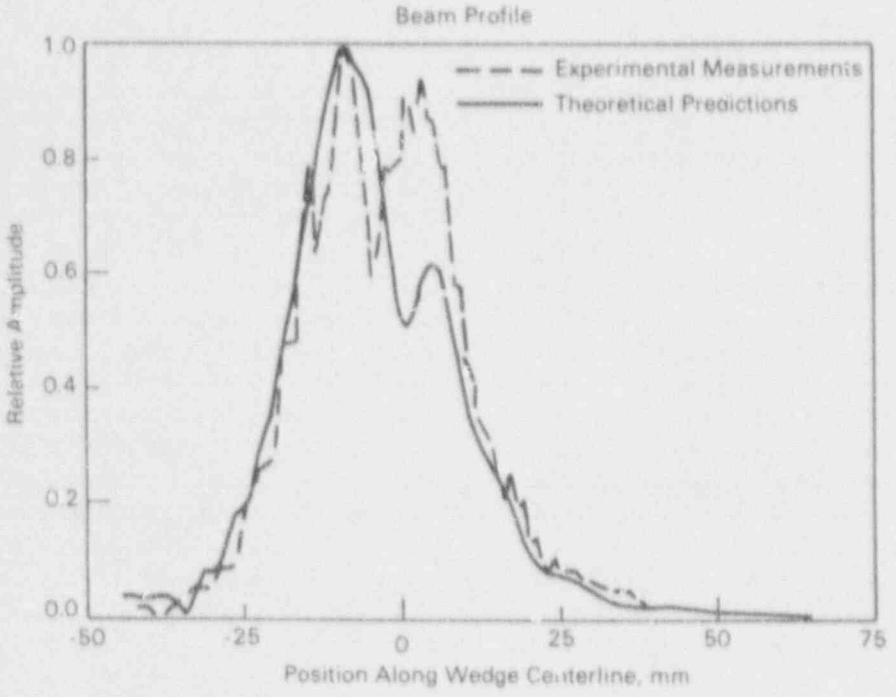

Figure 3.8. Predicted Versus Measured Sound Field along the Wedge Centerline at 1 MHz

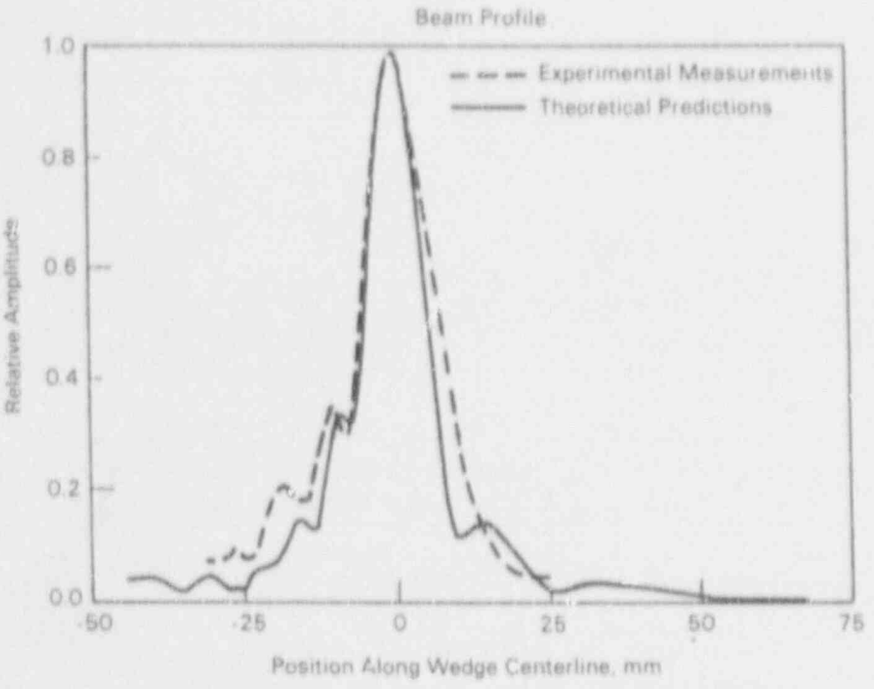

Figure 3.9. Predicted Versus Measured Sound Field along the Wedge Centerline at 2 MHz

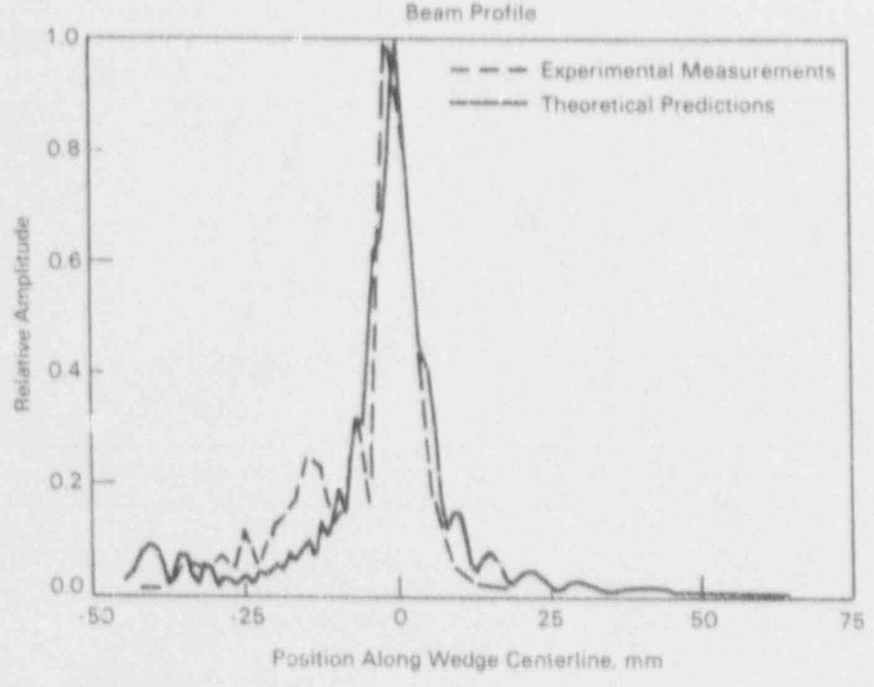

Figure 3.10. Predicted Versus Measured Sound Field along the Wedge Centerline at 5 MHz

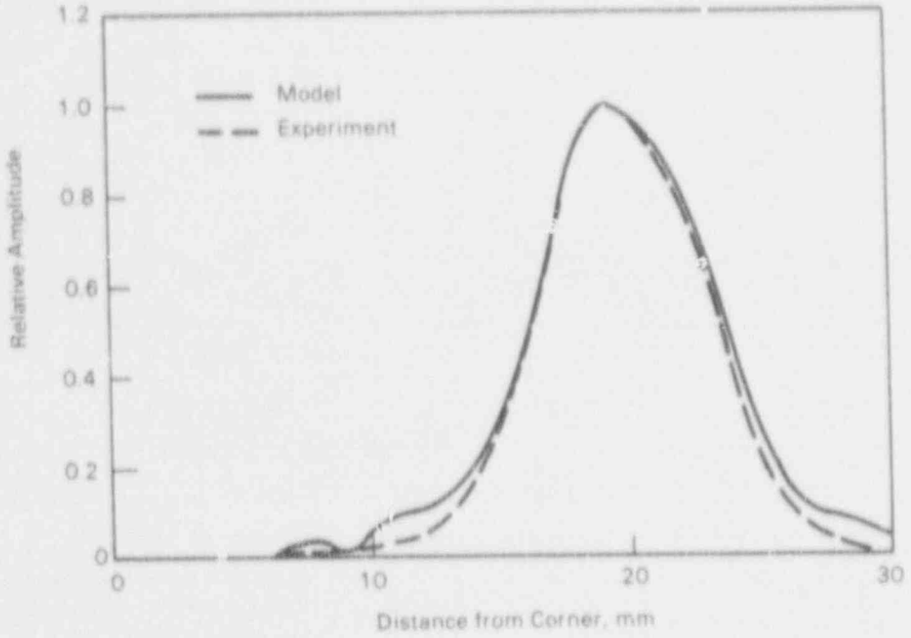

Figure 3.11. Predicted Versus Measured Pulse-Echo Response of a 90° Corner in a 20.8 mm Thick Steel Block at 5 MHz

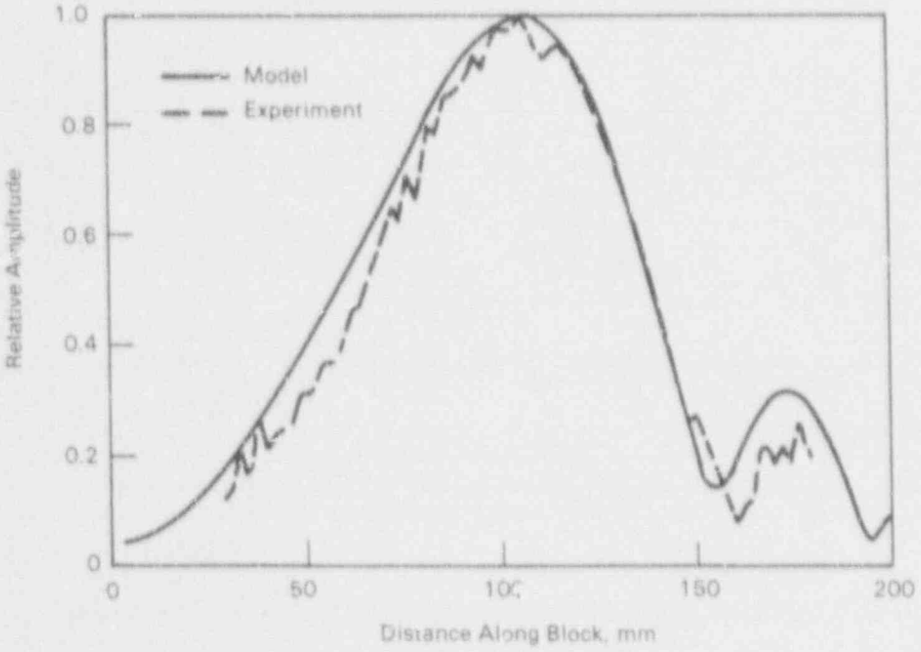

Figure 3.12. Predicted Versus Measured through Transmission Sound Field for 45° Longitudinal Wave Transmission through a 133-mm Thick Steel Block at 1 MHz

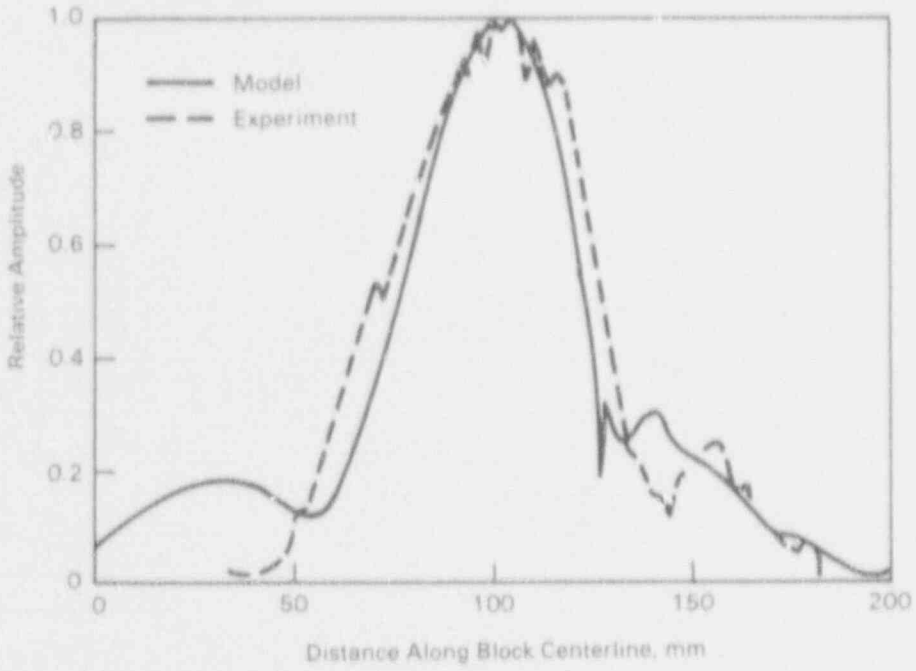

Figure 3.13. Predicted Versus Measured through Transmission Sound Field for 45° Transverse Wave Transmission through a 133-mm Thick Steel Block at 1 MHz

Experimental data from an independent source was used for the final set of single-frequency comparisons. PNL obtained tandem-probe inspection data taken at Risley and Harwell UKAEA laboratories (Murgatroyd et al. 1987) for the PISC-III program. Comparisons were made for specular reflection from the three defect types shown below in Table 3.1.

Table 3.1. Risley/Harwell Lab Defect Types

Defect Type	Tilt	Finish	Figure
25-mm diameter re-entrant machined flat-bottom hole	0°	Smooth	3.14
10 x 50-mm strip	0°	Smooth	3.15
25 x 125-mm strip	0°	Smooth	3.16

Comparisons for the strip defects were very favorable with only small offsets caused by small differences in probe angle. The model versus experiment comparison was not acceptable for the 25-mm flat-bottom hole. The 2-D PNL model performs well for specular reflection from strip defects, but it is not valid for defects whose length is smaller than the beam width.

To summarize, it was shown that at a single frequency the model is valid for specular reflection from essentially two-dimensional defects such as strip defects and 90° corners. The model did not prove to be valid for small circular defects.

Multifrequency pulse-echo measurements (more commonly known as ultrasonic spectroscopy measurements) were made on a set of aluminum blocks with the ends cut at various angles between 40° and 49° as shown in Figure 3.17. A very broadband ultrasonic system was used in conjunction with the computer-based ultrasonic spectroscopy system described in Doctor, et al. (1988) to determine transfer functions for the blocks. The block measurements represent specular reflections from large (100% through-wall), smooth

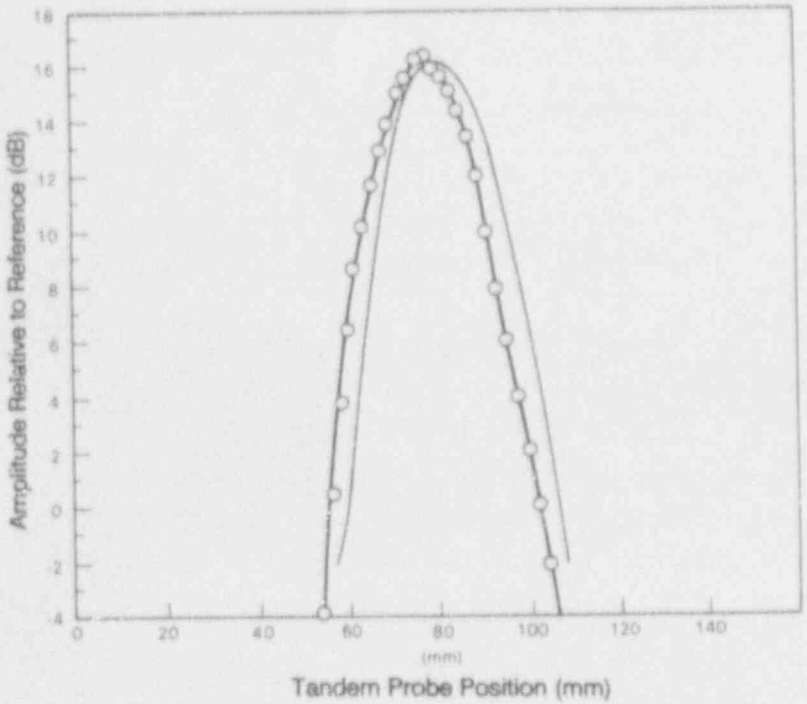

Figure 3.14. Predicted (Circles) Versus Measured Tandem Probe Scan Results for a 25-mm Flat-Bottomed Hole in a 193-mm Thick Steel Block at 2.25 MHz

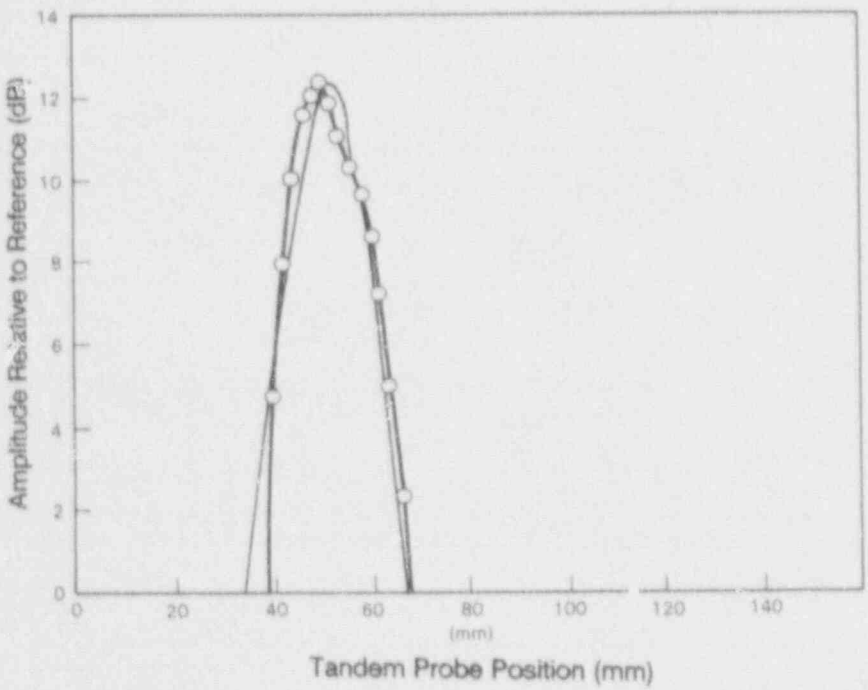

Figure 3.15. Predicted (Circles) Versus Measured Tandem Probe Scan Results for a 10-mm Strip Defect in a 193-mm Thick Steel Block at 2.25 MHz

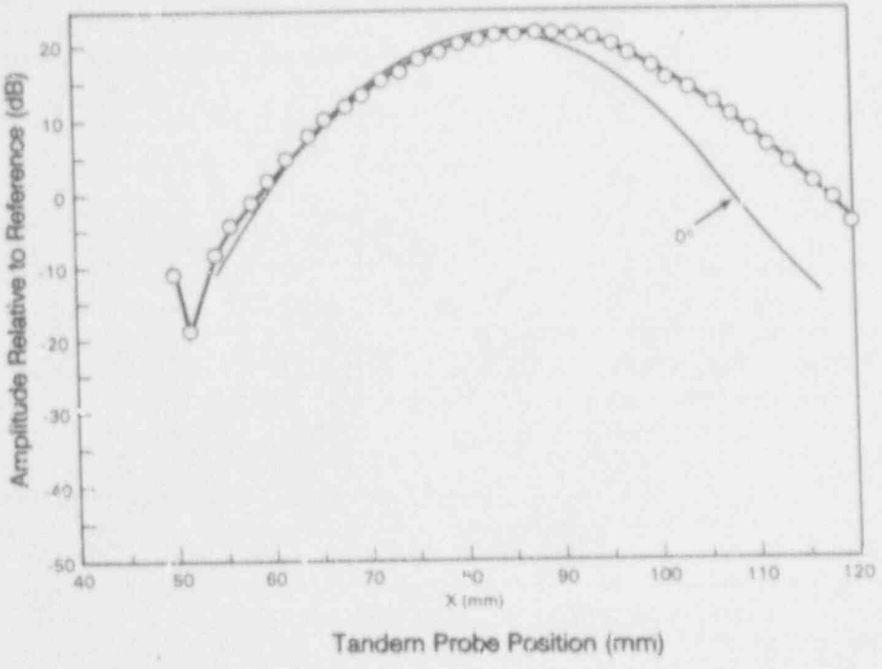

Figure 3.16. Predicted (Circles) Versus Measured Tandem Probe Scan Results for a 25-mm Strip Defect in a 193-mm Thick Steel Block at 2.25 MHz

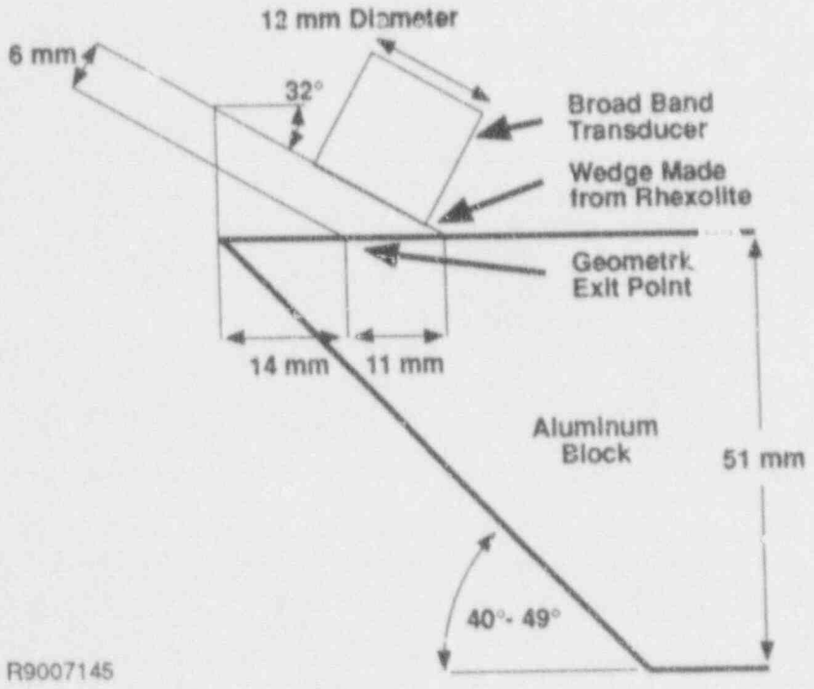

Figure 3.17. Configuration Used to Make Ultrasonic Spectroscopy Measurements

defects at various angles. Corresponding model calculations were made for comparison. A 12-mm (0.5-inch) transducer oriented to produce 45° vertically polarized shear waves was used, and these results cannot be generalized to transducers of other sizes and oriented at different angles. It is shown later in this report that transducer size affects the acoustic system transfer function very significantly.

Model versus experimental results are shown in Figures 3.18 through 3.26. The range of validity for the experimental measurements was 700 kHz to 6 MHz. In each case, the results were normalized with respect to the spectrum of the 45° block reflection. In general, the comparisons between experimental data and model predictions were good, but there were some differences.

Figure 3.26 shows the normalized transfer functions for the 49° block. Below 3 MHz, the measured transfer function is significantly greater in amplitude than the predicted result. This trend was also evident for the 48°, 47°, 42°, and 41° blocks; and it grew worse with greater deviation from 45°. This apparent amplification at low frequencies is currently unexplained, but the quality of the low frequency measurements is suspect.

The model did well in predicting the location of the first minimum in the acoustic system transfer function. Comparisons are made in Table 3.2. The ability to predict the minimum is of primary importance, since this feature distinguishes some defects as worst case. The response of a defect having a minimum at the inspection system's center frequency will be sensitive to bandwidth and center frequency changes and is, thus, considered a worst-case defect. The subject of worst-case defects with respect to equipment parameter changes is discussed in more detail later in this report. For the 12-mm (0.5-inch) transducer, the 41° and 40° blocks were predicted by the model to be worst-case defects for a typical 2.25 MHz inspection system, and the measurements confirmed this prediction. The model was completely successful in its ability to predict worst-case defects.

One last effect to notice is how much the transfer functions changed for a change of block angle of 1°. Part of this effect was due to measurement error, but much of it was real. This suggests that slight defect shape irregularities may have a significant impact on detection reliability.

Table 3.2. Comparison Between Predicted and Measured First Minimum in the Acoustic System Transfer Function

Angle Degrees	Measured MHz	Predicted MHz
49	3.5	2.75
48	4.0	3.5
47	4.5	5.0
46	None	None
44	None	None
43	5.75	5.5
42	3.5	4.0
41	2.5	3.0

To summarize, comparisons between measured data and model predictions confirmed the model's ability to predict worst-case defects. Differences between measured data and model results were not large compared to changes associated with slight angle deviations and repeatability errors.

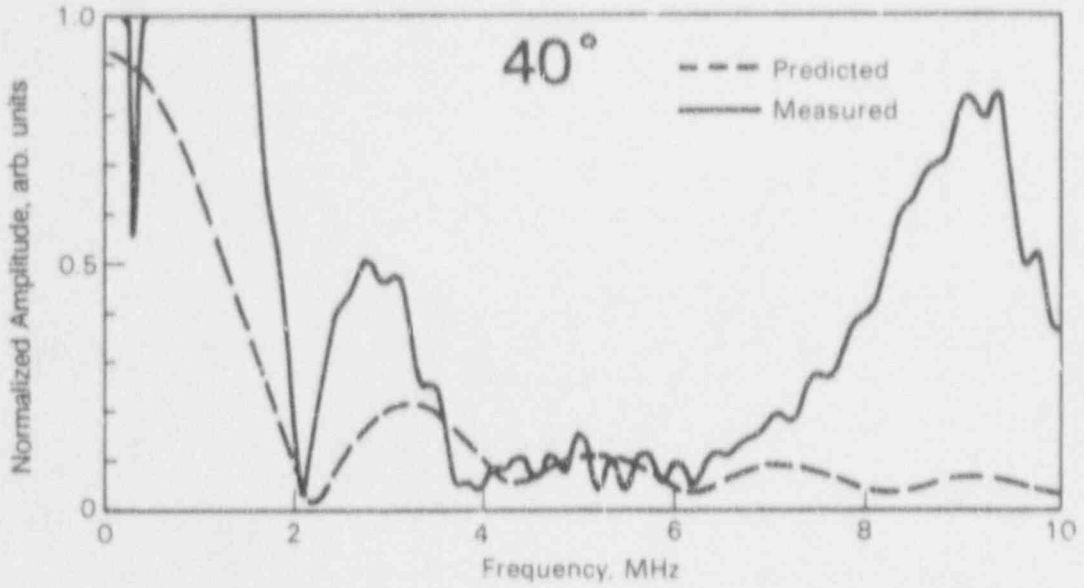

Figure 3.18. Predicted Versus Measured Acoustic System Transfer Functions for 40° Aluminum Block Normalized with Resect to the 45° Aluminum Block

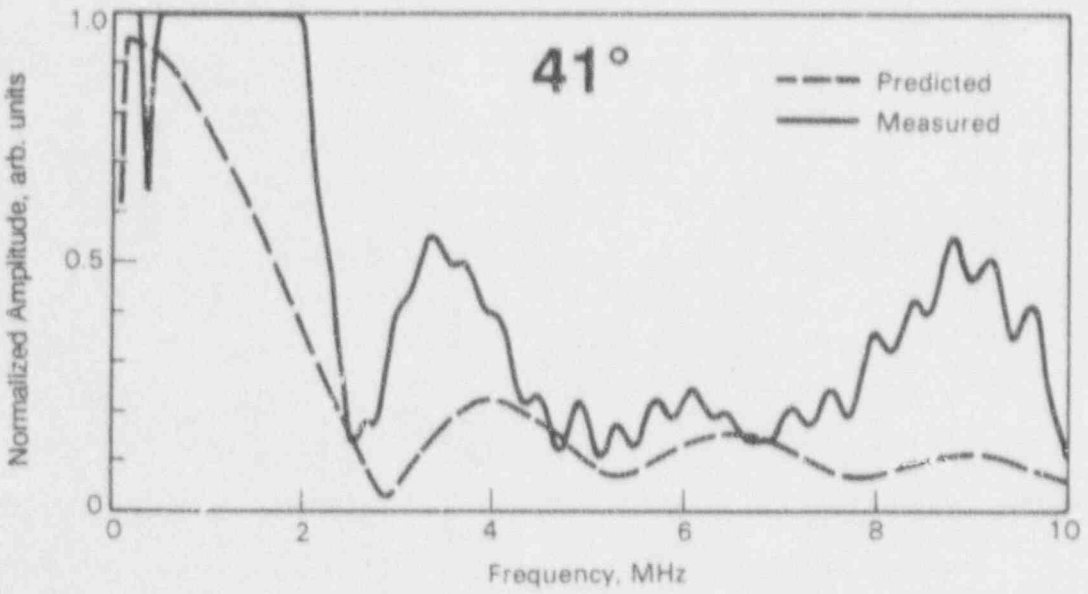

Figure 3.19. Predicted Versus Measured Acoustic System Transfer Functions for 41° Aluminum Block Normalized with Resect to the 45° Aluminum Block

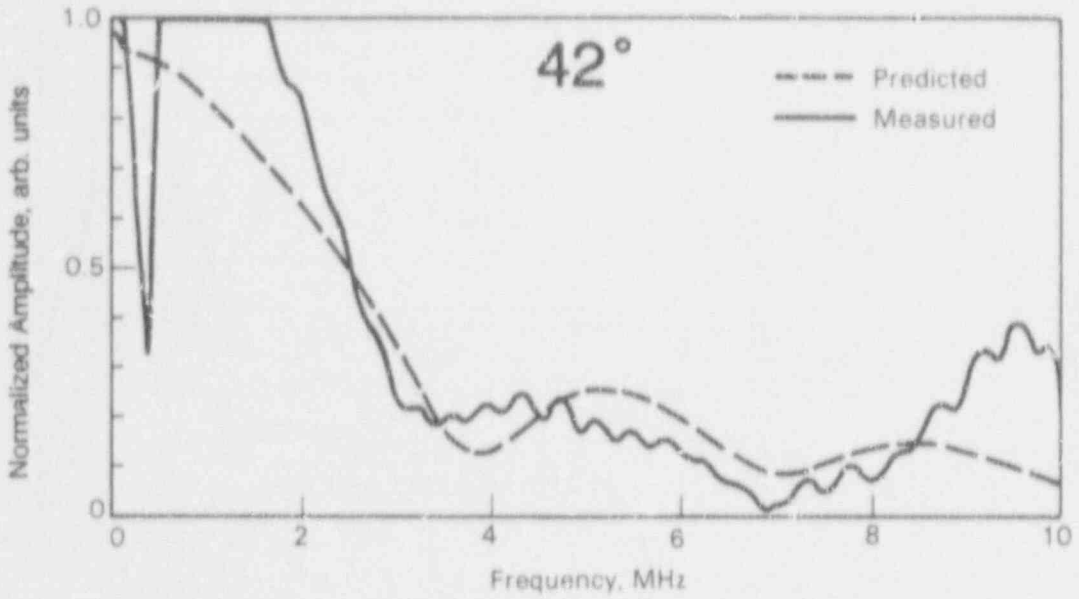

Figure 3.20. Predicted Versus Measured Acoustic System Transfer Functions for 42° Aluminum Block Normalized with Resect to the 45° Aluminum Block

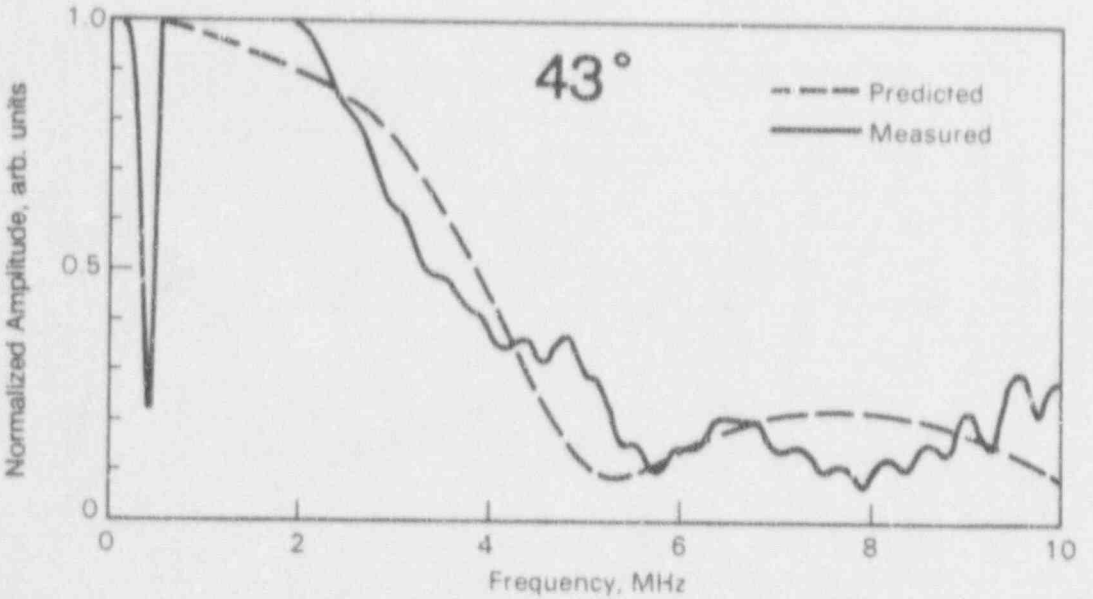

Figure 3.21. Predicted Versus Measured Acoustic System Transfer Functions for 43° Aluminum Block Normalized with Resect to the 45° Aluminum Block

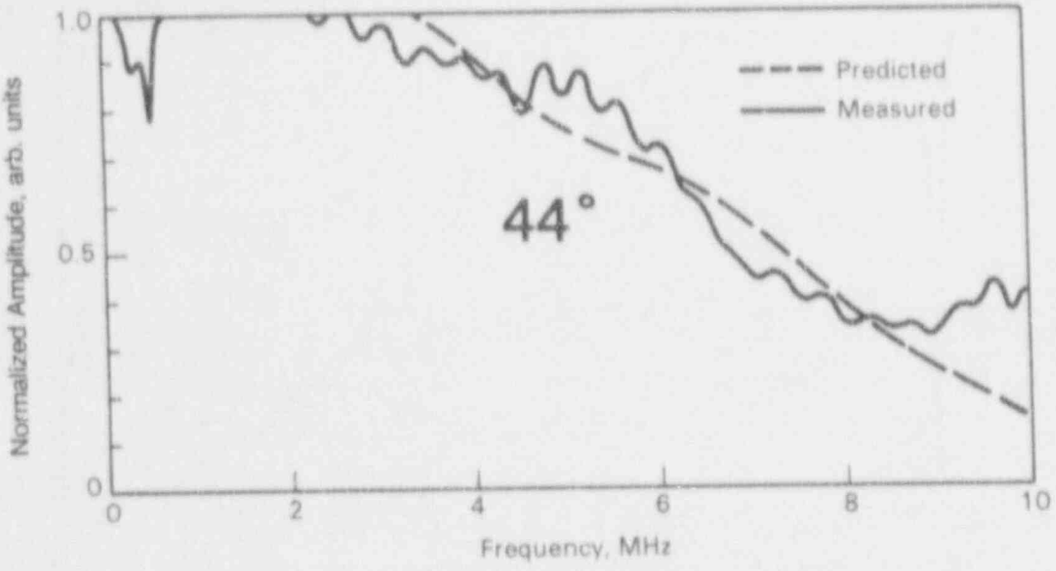

Figure 3.22. Predicted Versus Measured Acoustic System Transfer Functions for 44° Aluminum Block Normalized with Resect to the 45° Aluminum Block

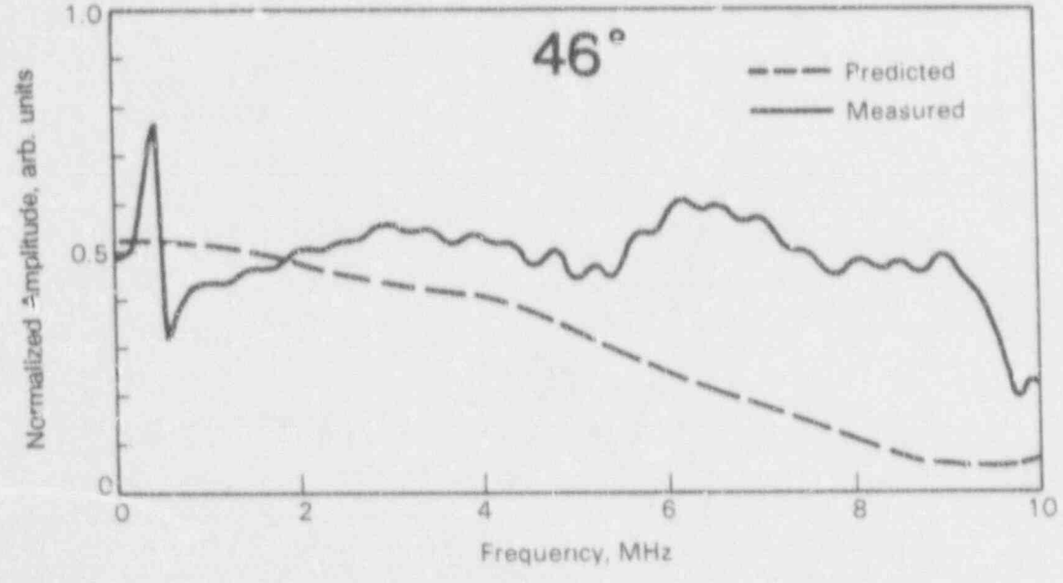

Figure 3.23. Predicted Versus Measured Acoustic System Transfer Functions for 46° Aluminum Block Normalized with Resect to the 45° Aluminum Block

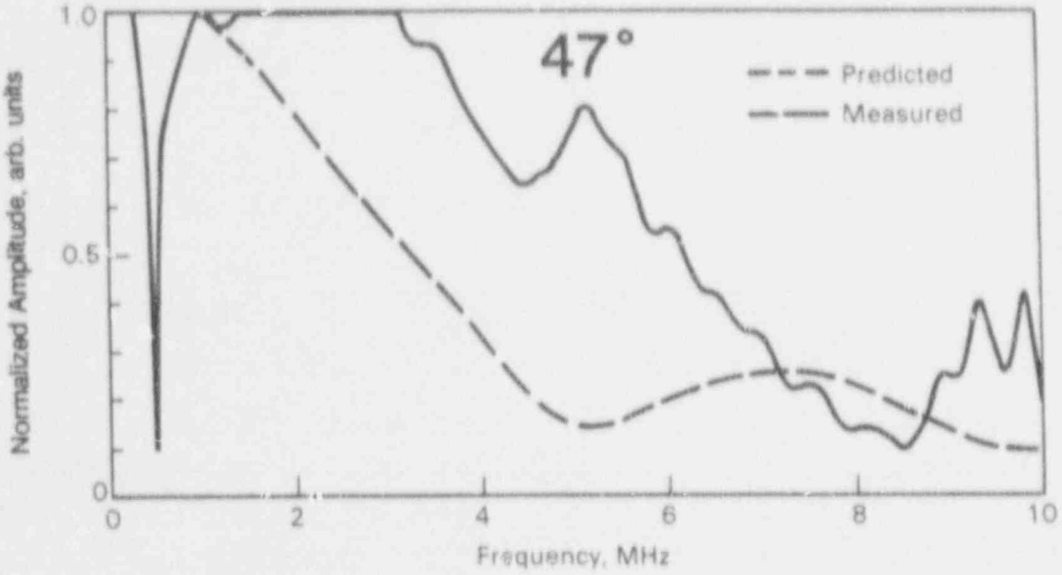

Figure 3.24. **Predicted Versus Measured Acoustic System Transfer Functions for 47° Aluminum Block Normalized with Resect to the 45° Aluminum Block**

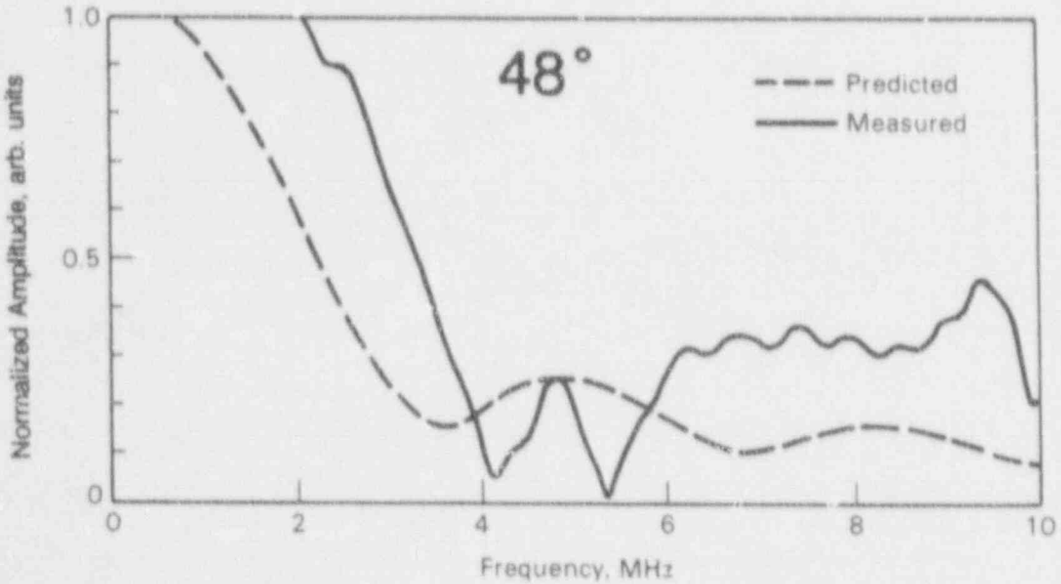

Figure 3.25. **Predicted Versus Measured Acoustic System Transfer Fuactions for 48° Aluminum Block Normalized with Resect to the 45° Aluminum Block**

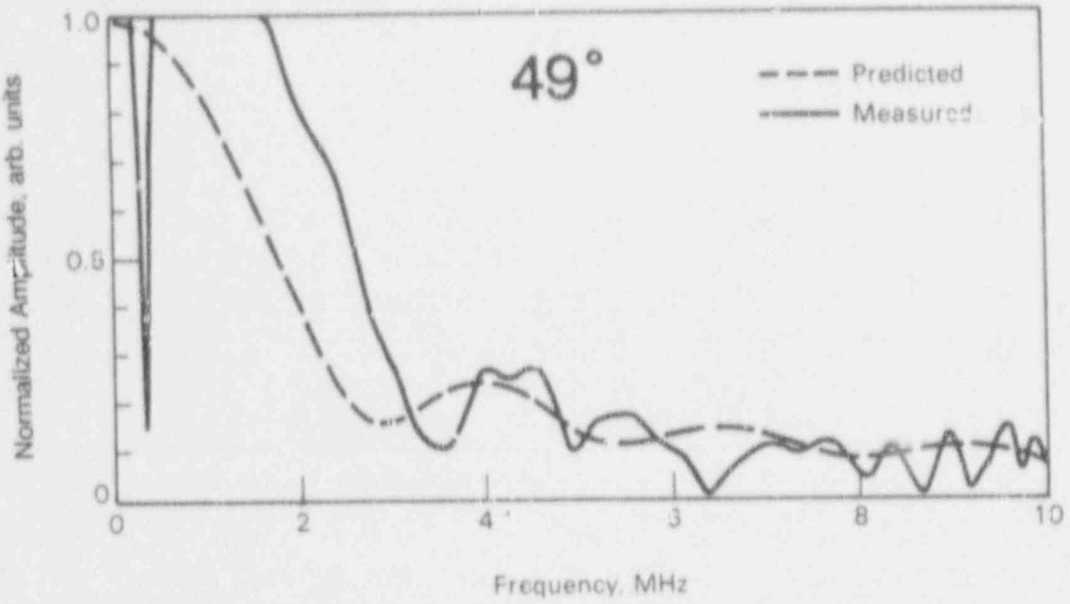

Figure 3.26. **Predicted Versus Measured Acoustic System Transfer Functions for 48° Aluminum Block Normalized with Resect to the 45° Aluminum Block**

4.0 Worst-Case Defects with Respect to Equipment Parameter Sensitivity

Coffey and Chapman (1983) and Coffey et al. (1982) considered what special properties a defect would have to have in order to ensure detection by ultrasonic inspection. In this report, a slightly different question pertaining to ultrasonic inspection reliability is considered, namely, what defect properties affect the repeatability of an ultrasonic inspection?

The acoustic systems associated with certain material defects can have frequency-domain characteristics that cause the echo amplitudes to differ significantly for ultrasonic inspection equipment of different bandwidths and center frequencies even when conventional calibration procedures are used. These differences reduce the reliability of defect detection and sometimes defect sizing (depending on the sizing method used). The effects of defect orientation, shape, size, roughness, and location on the acoustic system transfer function are discussed from the perspective of how they impact inspection reliability. Acoustic systems with characteristics that strongly reduce inspection repeatability [hereafter referred to as worst-case defect acoustic systems (WCDASs)] are identified, and strategies for identifying WCDASs and reducing their impact on ultrasonic inservice inspections are presented. Later in this report, WCDASs are used for the equipment parameter sensitivity studies to ensure that conservative tolerances are developed.

The problem of identifying WCDASs is a formidable one. The approach of modeling all possible acoustic systems and performing sensitivity studies to identify WCDASs is impractical as is the approach of collecting samples of all possible defects and performing experimental studies. Thus, two alternate approaches were taken. The ray tracing model was used to model acoustic systems within its scope (large, smooth, specular reflection). Also, the available literature was searched for data on acoustic systems that were too complicated for the model. This was done by looking at the expected frequency-domain interaction of the equipment and the acoustic system. Many papers have been written dealing with the ultrasonic frequency-domain response of materials and defects. This field is known as ultrasonic spectroscopy; a fairly comprehensive review of this subject can be found in Fitting and Adler (1981). These papers deal primarily with the use of ultrasonic spectroscopy as a tool for defect and material characterization; however, the plotted spectra are also approximations of transfer functions of the acoustic systems. Spectra taken from the available literature are used to estimate how those acoustic systems might interact with ultrasonic inspection equipment.

The effects of the variation of phase with frequency are ignored in this simple analysis. This decision was made for two reasons: 1) to simplify the analysis and 2) because almost no data exist in the literature on phase versus frequency for material defects. Admittedly, phase interaction between the equipment system and the acoustic system may prove to be significant (especially for rough defects), but phase interaction is not addressed in this report.

4.1 Frequency-Domain Interaction of Ultrasonic Inspection Equipment and the Acoustic System

To determine what features make an acoustic system a WCDAS, the interactions of the ultrasonic inspection equipment and the defect specimen are examined here in detail using simple, hypothetical transfer functions. The interactions of typical ultrasonic equipment-system spectra with several hypothetical acoustic-system transfer functions are illustrated in Figure 4.1. The following four cases are considered:

- Case A - a perfect notch filter
- Case B - a low-pass filter
- Case C - a rapidly oscillating sinusoid ($|\sin(x)|$)
- Case D - a sinc function ($|\sin(x)/x|$)

The calculated peak time-domain amplitude response from each of the combinations is summarized in Table 4.1.

As shown in Figure 4.1, the hypothetical perfect notch transfer function (Case A) interacts very differently with each of the three equipment systems in this example, producing responses with peak amplitudes ranging from 1 to -34.8 dB (see Table 4.1). From an equipment interaction point of view, Case A is a WCDAS. This type of transfer is highly sensitive to center-frequency and bandwidth changes for equipment systems with significant spectral content within the rejection band. Fortunately, acoustic system transfer functions like Case A do not exist in realistic inspection environments;

Table 4.1. Equipment and Acoustic System Interactions for Four Hypothetical Acoustic Systems

Transfer Function	Broadband Low Frequency, dB	Narrow Band Low Frequency, dB	Narrow Band High Frequency, dB
A - perfect notch filter	-4.0	-27.8	0.0
B - low-pass filter	-2.2	-2.2	-5.2
C - |sin(x)|	-3.9	-3.9	-4.0
D - |sin(x)/x|	-10.8	-23.7	-30.1

however, acoustic system transfer functions similar to those for Cases B, C, and D do exist, as will be seen later in this report.

The low-pass filter transfer function (Case B) is sensitive to center-frequency changes (the amplitude dropped from -2.2 to -5.2 dB in the example given in Table 4.1). The degree of center-frequency sensitivity depends on the slope of the transfer function. There is very little sensitivity to equipment bandwidth changes. In general, acoustic systems with smooth, continuous, and gently sloped transfer functions such as this are not WCDASs from an equipment-interaction point of view. However, they would be WCDASs, when the slope of the transfer function is steep.

The rapidly varying |sin(x)| transfer function (Case C) is insensitive to both equipment bandwidth and center-frequency changes (see Table 4.1). Acoustic systems with transfer functions that vary rapidly (at least twice per equipment bandwidth) and that have a gentle variation in smoothed amplitude are not WCDASs.

The Case D transfer function (|sin(x)/x|) is moderately sensitive to bandwidth changes (changed from -23.7 dB for narrow band to -10.8 dB for broadband in the example given in Table 4.1). The amplitude response of narrow-band equipment systems varies with frequency as the transfer function varies; therefore, narrow-band equipment systems would experience significant center-frequency sensitivity for acoustic systems with this type of transfer function, especially when the equipment center frequency is at or near a null in the transfer function. The center-frequency sensitivity decreases with increasing equipment bandwidth. An acoustic system with this type of transfer function is a WCDAS. Later in this report, an acoustic system with a transfer function of this form will be identified.

4.2 Frequency-Domain Characteristics of Various Defect Types

4.2.1 Defect Size and Angle and Probe Position

The changes in the acoustic system transfer functions due to defect orientation (tilt), defect size, and probe position were investigated using the simple ray-tracing model described earlier. The results are for specular reflection from smooth, planar defects, so the acoustic system transfer function variations are due to directivity of the piezoelectric source element, the receptivity of the receiving element, and subtle geometrical effects and not the defect directivity patterns. The modeled configuration is shown in Figure 4.2.

In Figure 4.3, the acoustic system transfer functions are plotted for corner reflection from various sizes of vertical defects (crack angle = 90°). The amplitude at each frequency is proportional to the defect size until the defect becomes larger than the insonifying beam, and none of the defects are worst case.

In Figure 4.4, acoustic system transfer functions are plotted for corner reflection from various sizes of nonvertical defects (crack angle = 85°). The amplitude at each frequency is no longer proportional to the

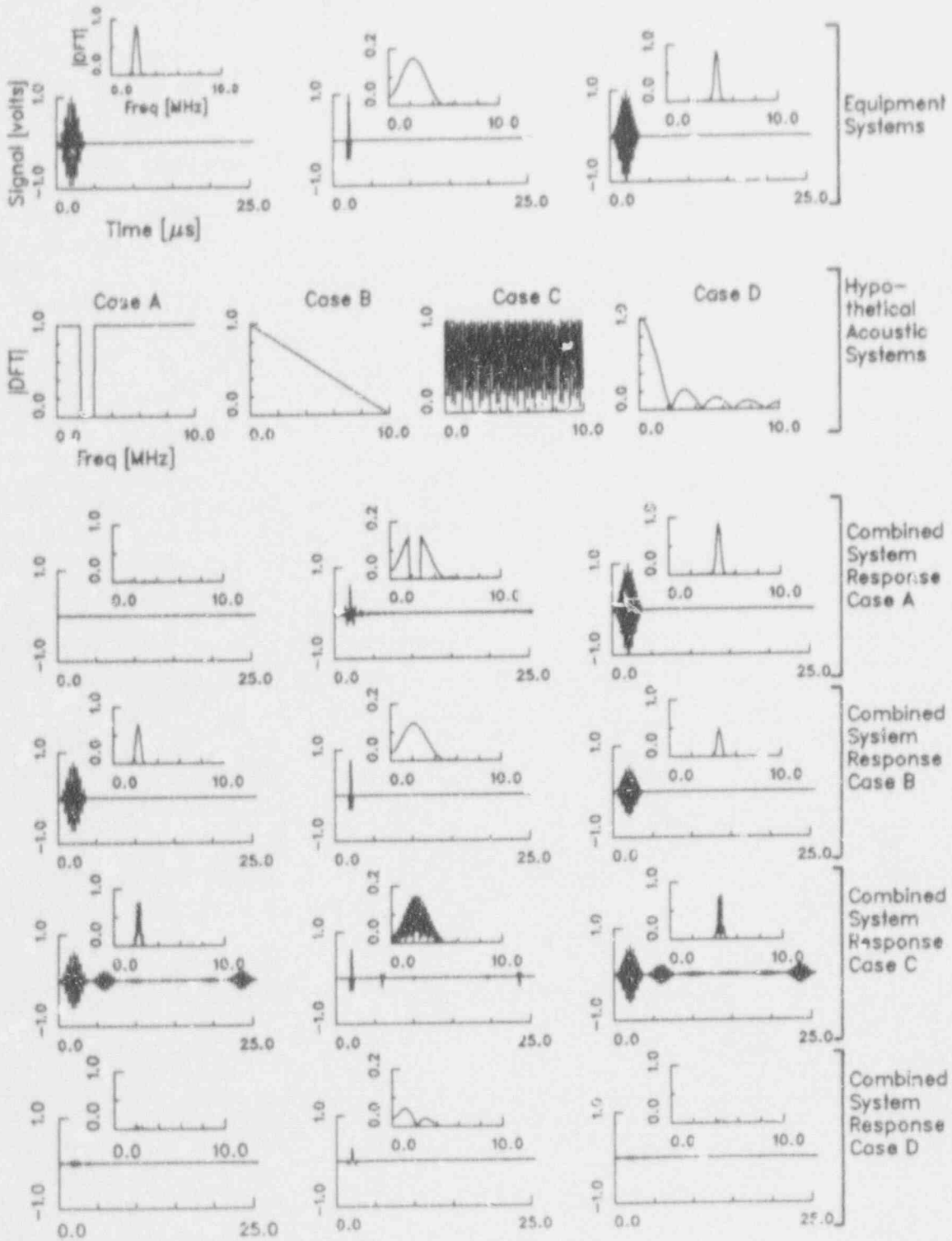

Figure 4.1. Equipment and Acoustic System Interactions for four Hypothetical Acoustic Systems

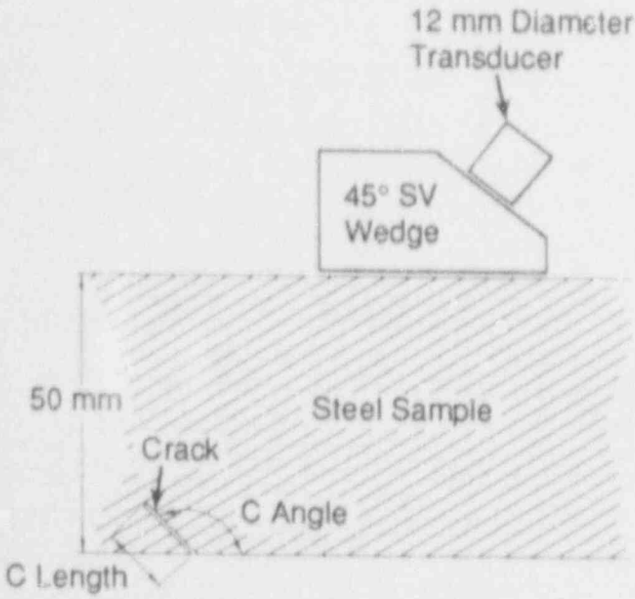

Figure 4.2. Pulse-Echo Ultrasonic Test Configuration

defect size, and most of these acoustic systems could be considered worst case for narrow band inspection systems. The larger defects also tend to have transfer functions with steeper slopes and more frequency minima than smaller defects, making larger defects of this type more sensitive to equipment changes.

Figure 4.5 shows acoustic system transfer functions for a small vertical defect with the pulse-echo probe at various locations. As the probe moves away from the maximum amplitude position (50 mm), the transfer function becomes worst case. These curves show that the repeatability of defect sizing methods that rely on the amplitude as a function of probe position may also be reduced by changes in equipment bandwidth and center frequency.

Using the ray tracing model, it was found that predicted, specular-reflection, acoustic-system transfer functions have minima due to phase differences in the sound incident on the receiving piezoelectric element. In other words, a response minimum occurs when the returning wavefront is not parallel to the piezoelectric element face so that half of the face is in tension and half is in compression. This effect is due to the phase sensitivity of piezoelectric receiving elements and was

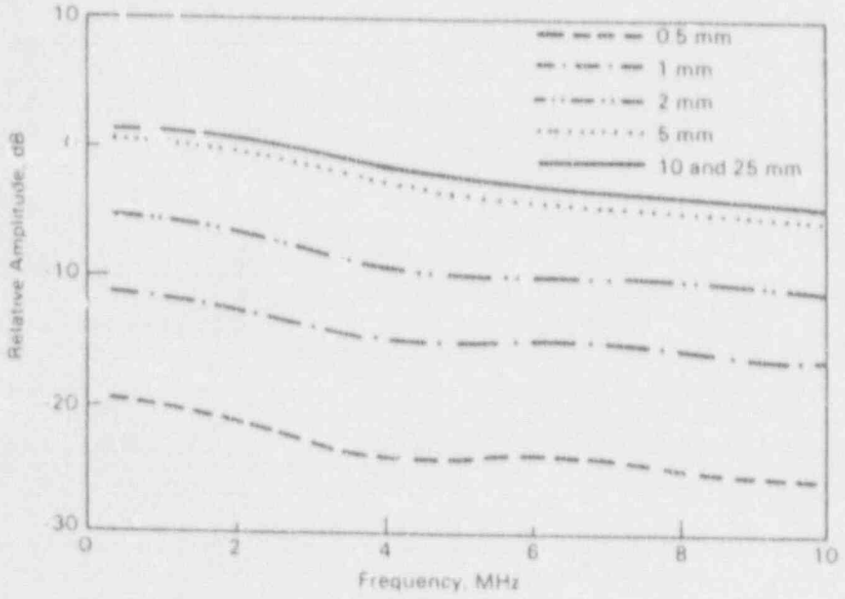

Figure 4.3. Frequency Response for Vertical Defects of Various Lengths

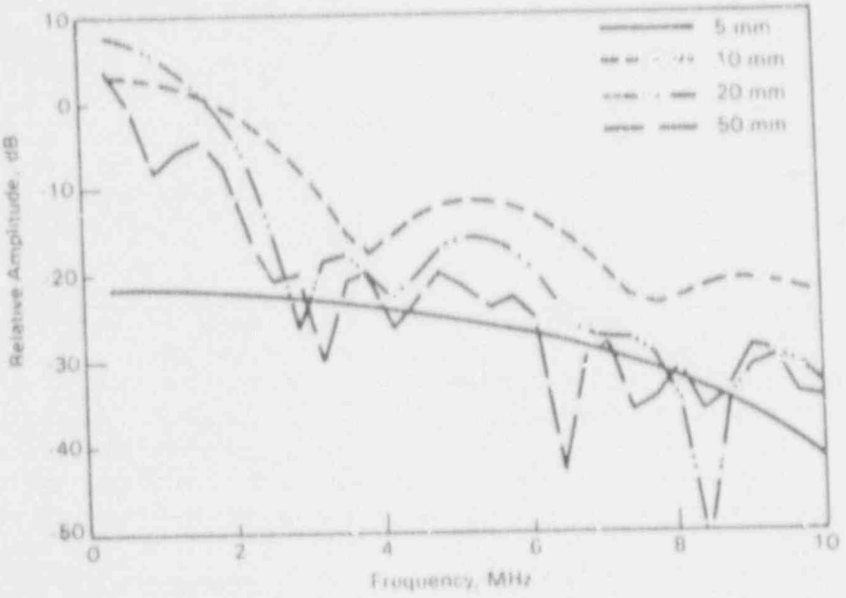

Figure 4.4. Frequency Response for 80° Defects

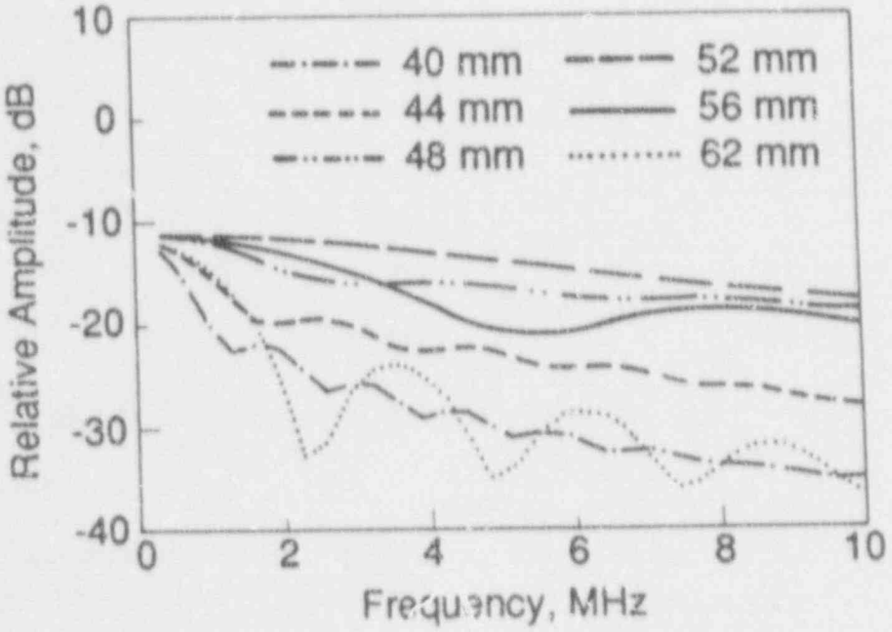

Figure 4.5. Frequency Response for 1-mm Vertical Defects for Various Probe Positions

also noted by Heyman and Cantrell (1977). Using this simple interpretation, the first acoustic system transfer function minimum occurs at the frequency, f_{min}, given by Eqn. (21).

$$f_{min} = \frac{c}{(d \cdot \sin\gamma)} \qquad (21)$$

where c is the speed of sound, d is the receiving element diameter, and γ is the angle between the received wavefront and the receiving element face.

The frequency domain features that make the WCDASs worst-case are produced by phase cancellation at the receiving piezoelectric element. Thus, the use of a phase-insensitive receiver would greatly decrease the sensitivity to equipment changes. Phase-insensitive receivers such as miniature hydrophones, zinc oxide, and cadmium sulfide (Heyman and Cantrell 1977) devices exist but are not generally commercially available.

When the inspection configuration does not allow for the reception of the specularly reflected wavefront, the received signal(s) can be thought of as being made up of a combination of sound diffracted by the edges of the defect. Adler et al. (1977) made ultrasonic spectroscopy measurements for reflection from smooth planar reflectors. The measured spectra were found to undulate, and the spacing between consecutive frequency maxima, Δf, was described by a purely geometrical interference model according to Eqn. (22).

$$\Delta f = \frac{c}{d \cdot \sin\theta + d \cdot \sin(\theta \pm \alpha)} \qquad (22)$$

where c is the speed of sound and d and θ are the reflector diameter and angle as shown in Figure 4.6. The angle between the transmitting and receiving transducers is α. The interference model assumes that the modulation in the spectrum is due to interference between wavelets produced by diffraction at the edges of the reflector. Also, as a simplification, the diffraction coefficients (both amplitude and phase) are assumed independent of frequency and incident angle. The wavefront incident on the reflector is assumed to be planar. Though these conditions are rarely met in practice, the Δf estimates are reasonably accurate as discussed in the original article (Adler 1977).

In general, if the interference between the edge diffraction wavelets is strong, the defect is worst-case with respect to equipment changes if Δf is comparable to the equipment bandwidth. If Δf is significantly smaller than the equipment bandwidth, there is a smoothing effect as seen in Case C in Section 4.1. If Δf is much larger than the equipment bandwidth, the slope of the acoustic system transfer function is less severe as in Case B in Section 4.1, and again the transfer function is not worst-case.

4.2.2 Defect Roughness

Jungman et al. (1977) made ultrasonic spectroscopy measurements for reflection from surfaces with a combination of random and periodic roughness profiles. The sample surfaces were prepared by successive engraving of a perfect grating and a random profile on lead blocks. The measurements were made by reflecting ultrasound at various backscatter angles from the sample surface immersed in water.

A typical measured spectrum from Jungman et al. (1977) consists of a rapidly alternating background level of approximately -30 dB with superimposed, strong peaks. It was shown that the peaks were due to the engraved grating and obeyed Bragg's Law.

Examination of the data in the article by Jungman et al. (1977) leads to the conclusion that the impact of defect roughness depends on the roughness profile. If the roughness is regularly spaced (as might occur in a fatigue crack), the acoustic system transfer function will be dominated by strong peaks with frequencies that depend on the feature spacing and the backscatter angle according to Bragg's Law. An acoustic system containing this type of defect would be considered worst case with respect to equipment changes for certain equipment systems. If the roughness profile is predominately random, the situation is much like Case C (see Table 4.1) and the acoustic system containing this type of defect would not be considered worst case.

4.2.3 Coarse-Grained Stainless Steel and Stress-Corrosion Cracking

In order to find equipment combinations to improve the detection of stress-corrosion cracks in coarse-grained stainless steel (CGSS), McElroy (1977) used ultrasonic inspection equipment combinations with a wide variety

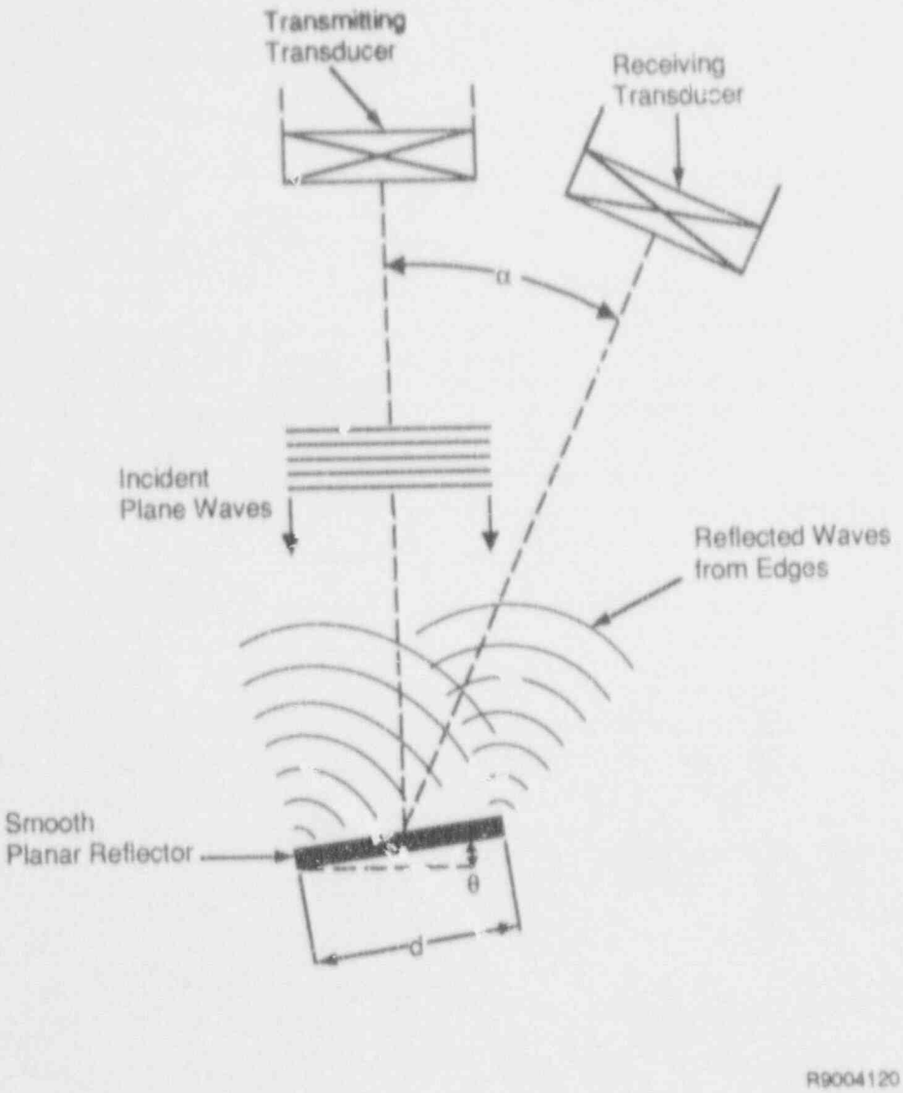

Figure 4.6. Schematic of the Interference Model

of center frequencies and bandwidths. Both the time-domain echo response and corresponding frequency-domain spectra were reported for 45° and 60° pulse-echo inspections. For each equipment combination, measurements were made for reflection from: 1) a 0.060-in. (1.5-mm) diameter side-drilled hole in a carbon steel IIW (International Institute of Welding) block; 2) the corner of a carbon steel IIW block; 3) the corner in the CGSS sample; and (4) a stress-corrosion crack in the CGSS sample. It was found that the CGSS produced very strong low-pass filtering with a cutoff frequency of approximately 1.8 MHz. Unfortunately, the grain structure was not described by McElroy, so the cutoff frequency cannot be correlated to grain size. The frequency-domain effect of the stress-corrosion crack was not apparent from the data given.

As discussed in the previous section on frequency-domain interaction, the degree of sensitivity to equipment center frequency changes depends on the slope of the acoustic system transfer function. Therefore, any CGSS acoustic system would be considered worst case if a significant portion of the equipment system spectrum was above the cutoff

frequency of the material. It is not clear if stress-corrosion cracks can generally be considered worst-case defects with respect to equipment changes.

4.3 Recognizing and Dealing with WCDASs

If the echo amplitudes of some types of acoustic systems are very sensitive to equipment parameter changes (in particular, center frequency), the field inspector would like to be able to identify these acoustic systems so that steps could be taken to ensure measurement reliability. Ideally, the inspector would identify the echo waveform of interest and compare its frequency spectrum with that of a suitable calibration reflector such as a 10% notch or a 90° corner. A change in the spectrum shape such as a strong low-pass filtering effect would identify the acoustic system as worst case.

Unfortunately, the field inspector does not have the luxury of having a spectrum analyzer and usually has only a limited amount of time to perform an inspection due to work schedules, radiation exposure, and/or inhospitable working conditions. Therefore, the inspector needs to be able to quickly identify a worst-case defect acoustic system based on the echo waveform. Such identification may be accomplished in the following ways:

1. A change in center frequency (as identified by the period) between the defect waveform and the calibration waveform would indicate that the acoustic system is acting as a strong low- or high-pass filter and is therefore a WCDAS.

2. Inspectors could perform sensitivity studies with three probes that differ only in center frequency (e.g., 2.0, 2.25, and 2.5 MHz). The inspector would examine the same defect with each search unit and note the change in the calibrated echo amplitude to determine the sensitivity of the acoustic system to equipment center frequency changes. The piezoelectric elements should be of similar manufacture and have equal diameters, and the wedges should be identical in material and physical dimensions. The actual inspection could be performed quickly if all three probes were calibrated in advance and if the appropriate instrument settings were noted in advance so that the setup could be changed quickly for each probe during the inspection.

In many ways, identifying WCDASs is easier than dealing with them. Some of the ideas developed in the previous sections suggest the following techniques for dealing with WCDASs:

1. When inspecting WCDASs, the inspection equipment should be fully characterized. When component changes are made, the equipment should be recharacterized to ensure equivalent performance. The ASME Code Section XI Appendix VIII provides tolerances for equipment component changes, but the inspector or engineer should recognize that meeting code requirements may not always ensure a repeatable inspection. For example, the two hypothetical spectra shown in Figure 4.7 are of typical equipment systems with equivalent bandwidth and center frequencies, but the shape of the spectra are different (perhaps because different types of transducer tuning circuits were used). For certain WCDASs, an unacceptable change in performance might result from going

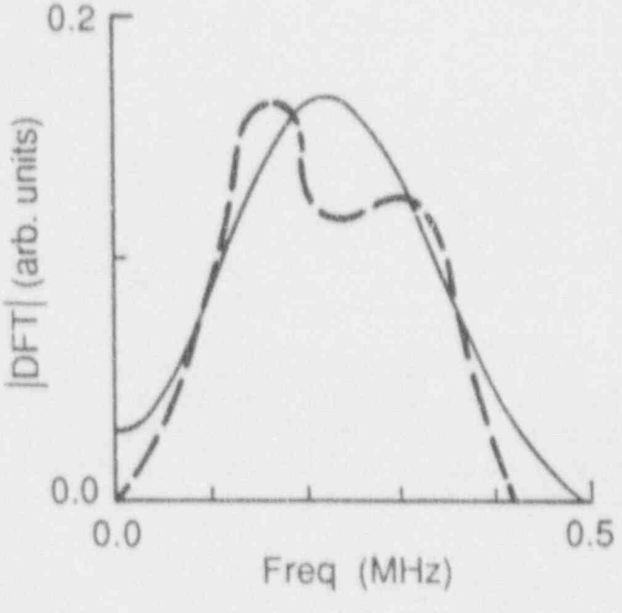

Figure 4.7. Hypothetical Equipment Spectra with Identical Bandwidths and Center Frequencies but Different Shapes

from one equipment system to another. To maximize repeatability with WCDASs, the inspector might:

- use a replacement transducer of the same size and shape
- use a replacement wedge of identical material and physical dimensions
- match the replacement equipment system spectrum to the original equipment system spectrum in bandwidth, center frequency, and shape; examine the equipment spectrum by using the echo from a suitable broad-band calibration reflector. The general shape of the waveform produced by the replacement system should also be similar to that of the original system. More work is required to define how closely the replacement system spectrum should match that of the original system to ensure a repeatable inspection.

2. Because of frequency-domain filtering effects, the echo amplitudes of WCDASs are almost always lower than those of similarly sized non-worst-case defect acoustic systems; therefore, another way of dealing with worst-case defects is to lower the detection threshold levels.

3. The inspector could use the same equipment each time the defect is inspected, although this might prove difficult for periodic inspections spanning months or years (e.g., monitoring the growth of a crack that is smaller than critical size), because transducers and cables must commonly be replaced due to loss or damage.

4. Usually, the use of broad-band equipment reduces the sensitivity of the equipment system when inspecting WCDASs. It should be noted, however, that broad-band equipment systems usually have lower sensitivity, thus reducing the signal-to-noise ratio.

5. The inspector could try another probe. As discussed earlier, the acoustic system transfer function depends on the configuration of the probe (piezoelectric element and wedge angle) as well as the configuration of the defect. Changing the wedge angle or reducing the diameter of the receiving piezoelectric element may reduce the sensitivity to equipment parameters. The inspector could also try a special phase-insensitive receiving probe. This technique may also help identify the type of material defect because the way that the calibrated echo responds to reducing the phase-sensitivity of the receiving element provides some evidence about the nature of the defect. For example, the specular reflection from a nonvertical, smooth, and flat defect (such as a thermal fatigue crack) should be much less sensitive to equipment center frequency changes after switching to a phase-insensitive receiving element. Conversely, a waveform made up of two overlapping crack tip signals may remain sensitive to equipment center frequency changes even after switching to a phase-insensitive receiving element.

5.0 Sensitivity Studies

As discussed in the previous section, the transfer functions of worst-case defect acoustic systems (WCDASs) have a shape that makes the inspection results sensitive to equipment system bandwidth and center frequency changes. Using the previously described ray tracing model, postulated WCDAS (Table 5.1) transfer functions were calculated for various combinations of material thickness, transducer size, and defect angle. The defect angle was varied until a minimum occurred at 2.25 MHz. In preliminary sensitivity studies, this shape was found to be approximately the worst for center frequency and bandwidth sensitivity. Sensitivity studies were not run to optimize the WCDAS transfer functions, as the time required would be prohibitive. The transfer functions (Figures 5.1 and 5.2) are used in the sensitivity studies that follow. Note that the transfer functions act as low pass filters. Other types of defects have transfer functions that make inspection results sensitive to equipment changes, but large, smooth defects are believed to be the worst.

The percent bandwidth is defined according to Eqn. 5.1.

$$B.W.\ (percent) = \frac{(f_h - f_l) \times 100}{f_c} \qquad (23)$$

where f_c is the peak frequency of the spectrum, f_l and f_h are the lower and upper frequencies, respectively, at which the spectrum is at 50% of peak.

ASME requirements do not contain tolerances for measurement repeatability, so adequate measurement repeatability is defined here as ±2 dB (±26%). The 2 dB criterion was chosen after discussions between PNL staff and ASME Code members. A combination of changes (e.g., a 10 % change in bandwidth plus a 10% change in center frequency) is worth considering here. If the allowable change in echo amplitude due to a bandwidth change is 2 dB and due to a center frequency change is 2 dB, the possibility exists that the echo amplitude could change 4 dB. It is also possible that the bandwidth and center frequency changes could cancel leaving the echo amplitude unchanged after the equipment replacement.

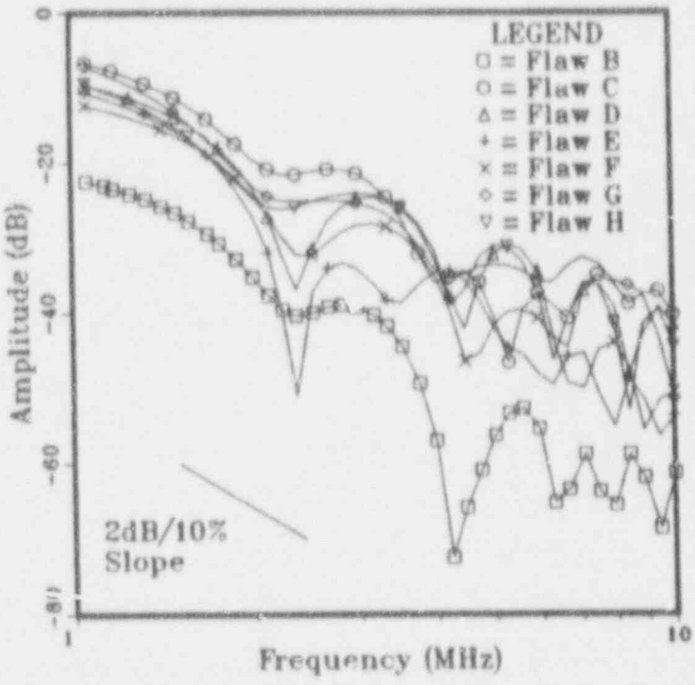

Figure 5.1. Calculated Transfer Function for Seven Postulated WCDASs for 45° SV Inspection. Curves are not normalized with respect to one another.

5.1 Modeling Bandwidth Sensitivity Study - 45° SV Inspection

An equipment bandwidth sensitivity study was conducted by convolving the worst-case defect impulse responses (the inverse Fourier transform of the transfer functions) with waveforms representative of ultrasonic inspection systems with bandwidths ranging from 273 kHz (12%, very narrow-band) to 3.48 MHz (155%, very broadband). In each case, the equipment center frequency remained at 2.25 MHz.

In Figure 5.3, one curve of normalized amplitude versus bandwidth is plotted for each postulated worst-case defect. The results in Figure 5.3 indicate that a bandwidth change of 10% would produce a calibrated echo response change of less than 2 dB for the seven postulated worst-case defects considered (i.e., none of the curves in Figure 5.3 are steeper than the 2 dB/10% slope reference line). If the bandwidth tolerance was

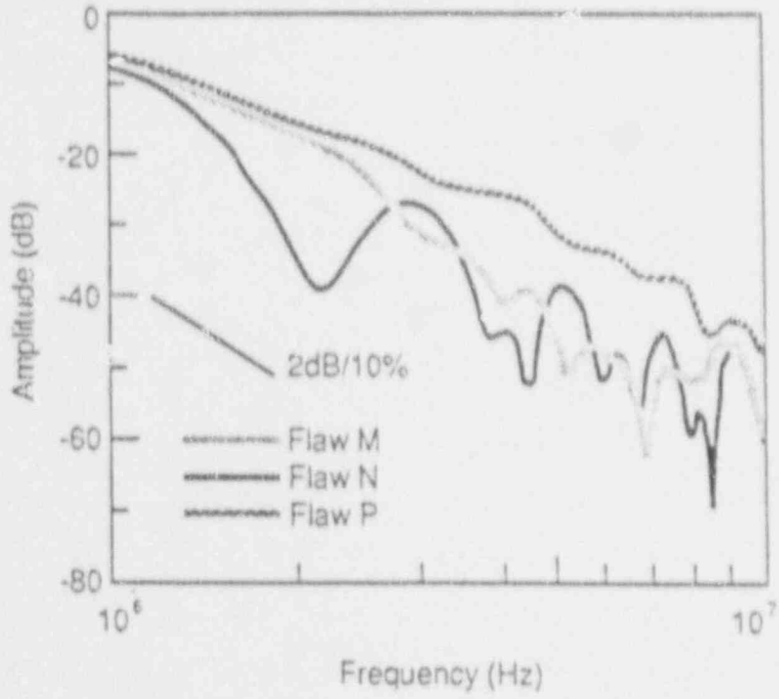

Figure 5.2. Calculated Transfer Functions for Three Postulated WCDASs for 60° SV Inspection
Curves are not normalized with respect to one another.

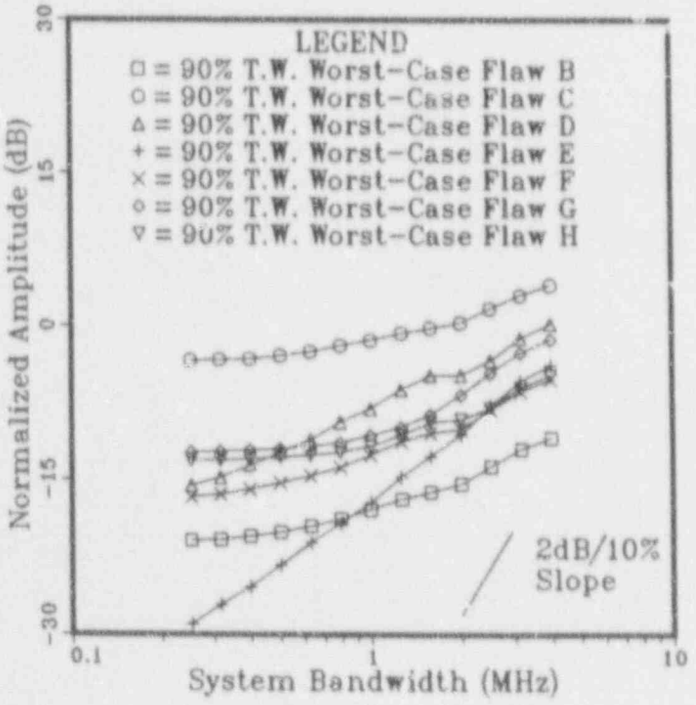

Figure 5.3. Bandwidth Sensitivity Study Results for Seven Postulated WCDASs for 45° SV Inspection

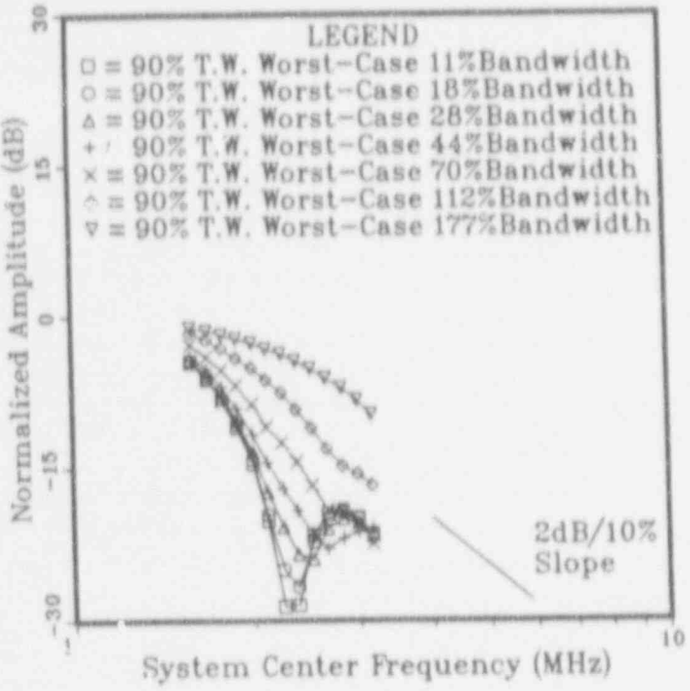

Figure 5.4. Center Frequency Sensitivity Study Results for Worst-Case Defect E

Table 5.1. Postulated WCDASs for Sensitivity Studies

Name	Probe Size	Material Thickness	Percent Through-Wall	Angle from Vertical	Inspection Type
Defect B	6 mm	19 mm	90%	-57°*	45° SV
Defect C	12 mm	19 mm	90%	6.5°	45° SV
Defect D	12 mm	19 mm	90%	-48°	45° SV
Defect E	12 mm	76 mm	90%	6.5°	45° SV
Defect F	12 mm	76 mm	90%	-49°	45° SV
Defect G	25 mm	76 mm	90%	3.5°	45° SV
Defect H	25 mm	76 mm	90%	-45.5°	45° SV
Defect M	12 mm	19 mm	90%	13°	60° SV
Defect N	12 mm	76 mm	90%	11°	60° SV
Defect P	25 mm	76 mm	90%	5°	60° SV

*Minus sign indicates that defect is angled away from the inspection probe.

relaxed to a less conservative value of ±20%, a ±2 dB repeatability could still be maintained according to this model study; but it should be recognized that defects whose inspections are more sensitive to equipment bandwidth changes than the postulated worst-case defects used in this study may exist so that some extra margin should be maintained. It should also be noted that the ASME bandwidth equipment tolerance pertains to individual inspection system components (e.g., the transducer) and not the entire inspection system as considered here. This should present no problem, since the change in system bandwidth should be equal to or smaller than the change in bandwidth of the component. Thus, this model study suggests that the ASME requirement of ±10% for component bandwidth changes is sufficient.

5.2 Modeling Center Frequency Sensitivity Study - 45° SV Inspection

In the center frequency sensitivity study the effect of equipment center frequency changes about a nominal value of 2.25 MHz was determined for various postulated worst-case defect and equipment bandwidth combinations. Center frequency sensitivity calculation results for the worst of the seven postulated worst-case defects (defect E) are plotted in Figure 5.4.

The results in Figure 5.4 indicate that none of the systems considered would be repeatable to within 2 dB after a center frequency change of 20%. The results suggest that a center frequency tolerance of ±10% is not sufficient for inspection systems with bandwidths less than 150%. A tolerance of 3.5% is indicated for systems with bandwidths between 20% and 100%. Systems with bandwidths less than 20% may be too sensitive to center frequency changes to permit repeatable inspection of worst-case defects. To put these results in perspective, the typical bandwidth of modern field inspection, piezoelectric transducers is approximately 50%. High resolution, field inspection transducers have bandwidths as high as 100%. Typically, only laboratory systems have bandwidths greater than 100%. High penetration, tone burst inspection systems can have bandwidths of 20%.

5.3 Modeling Bandwidth Sensitivity Study - 60° SV Inspection

In many applications the source of an inspection system will operate with either 60° or 45° shear waves. Therefore, the same sensitivity study discussed above for 45° shear waves has been repeated for 60° shear waves. Increasing the shear wave angle by 15° should not alter the fundamental sensitivity of the system equipment parameters: however, it is necessary to investigate all possibilities of the model for completeness.

Three defects (C, E, and G) from Table 5.1, considered to be worst-case in the 45° shear wave study, were selected for further investigation with 60° shear waves. Each of these defects (M, N, and P) can be found in Table 5.1, along with their geometry and general characteristics. The angle from vertical for each defect was varied until the calculated transfer function (Figure 5.2) indicated maximum sensitivity to inspection system equipment parameter changes.

An equipment bandwidth sensitivity study was conducted for 60° shear waves using the same analysis as described above for 45° shear waves. Figure 5.5 displays the normalized amplitude versus bandwidth plotted for each of three postulated worst-case defects; while Figure 5.6 shows the system sensitivity to changes in bandwidth (slope) calculated from the curves in Figure 5.5, and plotted in dB per 10% change in system bandwidth frequency at six different frequency values.

As reported in the 45° study, the model predicts a ±2dB repeatability could be maintained even when the bandwidth tolerance is relaxed from its current Code value of 10% to a less conservative value of about 20%.

5.4 Modeling Center Frequency Sensitivity Study - 60° SV Inspection

The center frequency sensitivity was studied for the effect of equipment center frequency variations about a nominal value of 2.25 MHz using 60° shear waves exactly as previously discussed for 45° shear waves. Results are displayed in Figures 5.7 and 5.8 for one (defect N) of the three postulated worst-case defects.

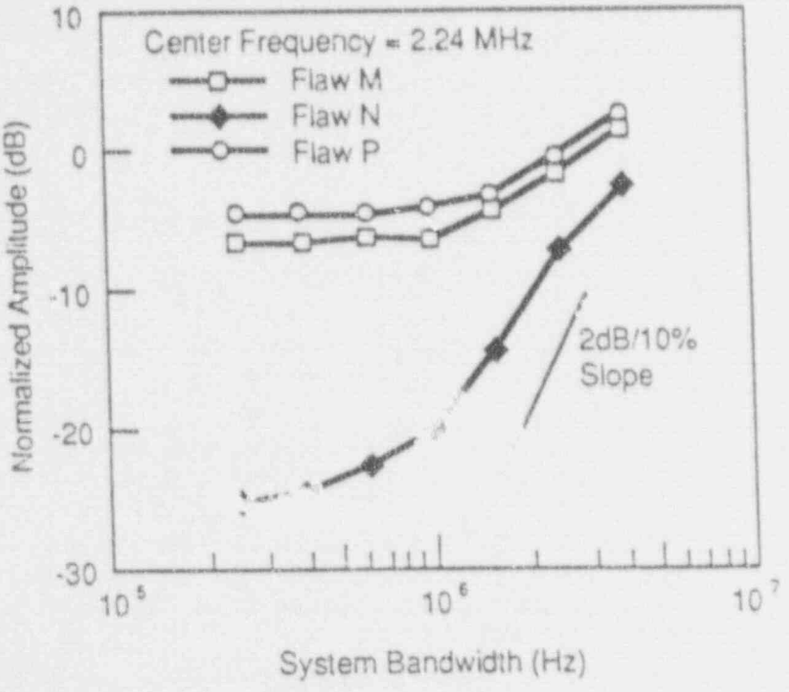

Figure 5.5. Bandwidth Sensitivity Study Results for Three Postulated WCDASs for 60° SV Inspection

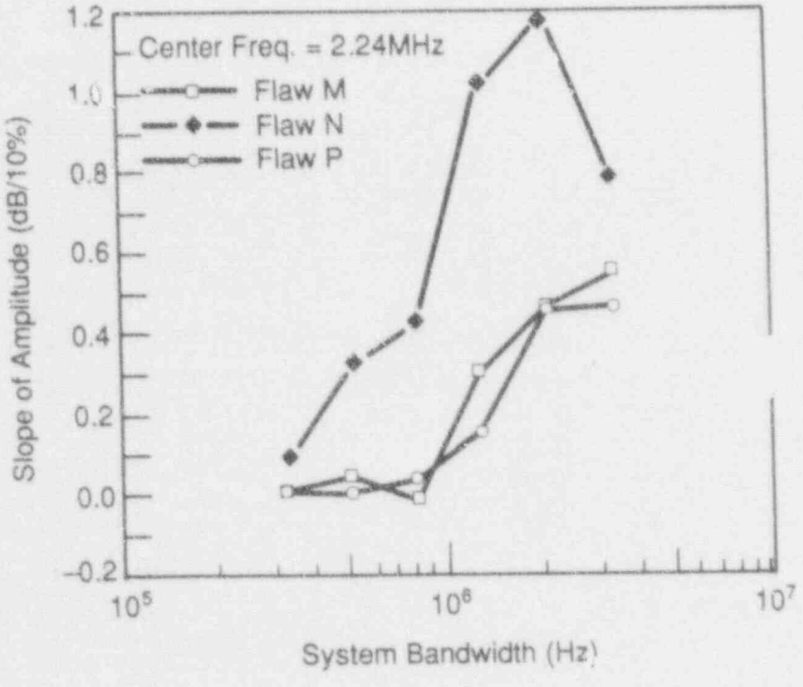

Figure 5.6. Slope of Bandwidth Sensitivity Curves for Three Postulated WCDASs for 60° SV Inspection

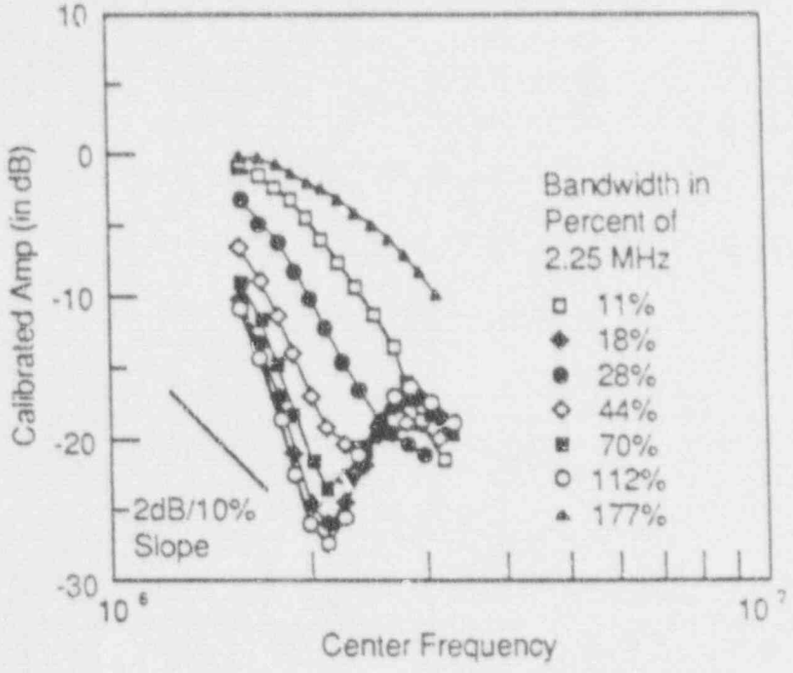

Figure 5.7. Center Frequency Sensitivity Study Results for Worst-Case Defect N

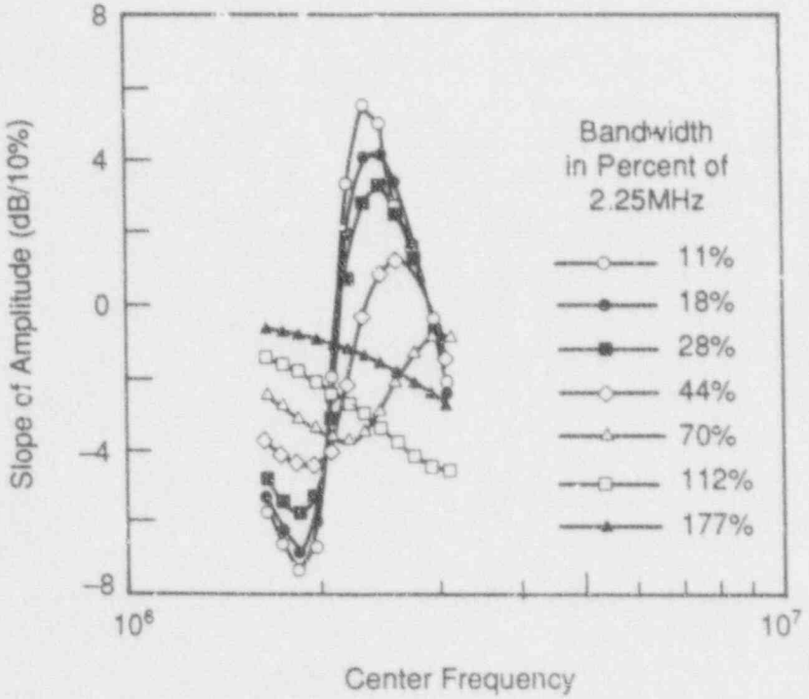

Figure 5.8. Slope of Center Frequency Sensitivity Curves for Worst-Case Defect N

Figure 5.7 suggests the response to center frequency variations of 60° shear waves is very similar to that found for 45° shear waves. However, Figure 5.8 shows the slope of two curves in Figure 5.7 to be slightly larger for the 60° case than computed for the 45° study. More specifically, curves representing 11% and 28% bandwidths resulted in about 2dB per 10% frequency change more sensitive. As found in the 45° study, a tolerance of ±3.5% appears more appropriate for inspection systems with bandwidths between approximately 20% and 100%.

5.5 Experimental Center Frequency Sensitivity Study

The conclusion that the ASME code center frequency tolerance of ±20% may not be sufficient to ensure repeatable inspection of worst-case defects is very significant and warrants further investigation, so an experiment was performed to test the center frequency sensitivity of worst-case defect inspection. Existing samples were pre-screened using broadband ultrasonic spectroscopy measurements to find worst-case samples with spectra that suggest the samples would be sensitive to center frequency changes. The samples do not correspond to the postulated worst-case defects considered above.

In the experiment, the echo responses from seven transducers of similar manufacture but with different center frequencies (1.0, 1.5, 1.8, 2.0, 2.25, and 5 MHz) were recorded. Two transducers with a center frequency of 2.25 MHz were used to provide statistical data on measurement variation. The echo responses were obtained for 45° SV, pulse-echo, contact inspection of six artificial defects including worst-case defects (those expected to have a high sensitivity to inspection system center frequency changes) and control defects (those not anticipated to be sensitive to center frequency changes). The defect specimens are described in Table 5.2. The defects in the 15-mm thick samples were circular saw cuts.

The data from the experiment is plotted as squares and crosses in Figures 5.9 and 5.10. A maximum allowable sensitivity of 2 dB/10% was chosen as discussed above. Examination of Figures 5.9 and 5.10 reveals that none of the three worst-case defects had center frequency sensitivities greater than 2 dB/10%; thus, the center frequency sensitivity of the worst-case defects tested was acceptable. The control defects displayed no significant center frequency sensitivity.

All of the transducers tested were relatively broadband yielding system bandwidths of approximately 70% except the 5 MHz transducer which produced a system bandwidth of 149%. The modeling studies showed that broadband systems are significantly less sensitive to center frequency changes than narrow-band systems, so the experimental data was artificially narrow banded to simulate the response of narrow-band systems with various center frequencies. The response was narrow banded by taking the amplitude of the response spectrum and low-pass filtering the spectrum above the system center frequency and high-pass filtering below the system center frequency. The inverse Fourier transform of the filtered spectrum was taken to get the artificially narrow-banded time response. Filter slopes of 90 and 130 dB/decade were used, resulting in system bandwidths of approximately 28% and 19%, respectively.

The artificially narrow-banded results are plotted in Figures 5.9 and 5.10. The center frequency sensitivities of the 55° Al block and defect Q increased significantly with narrow banding. The center frequency sensitivity for the narrow-band systems is approximately 4 dB/10% which is unacceptable per the 2 dB/10% limit that has been adopted for this report. A center frequency tolerance of ±5% appears to be more appropriate for the 20% and 28% inspection systems.

The ASME requirement of ±20% is not sufficient to guarantee inspection repeatability to within 2 dB for typical inspection systems (bandwiths between 20% and 100%).

The experimental results are in general agreement with the modeling results, but the experimental results do not exhibit as much sensitivity to equipment center frequency changes as the modeling results. More work needs to be done to determine if the model is overly conservative.

Table 5.2. Experiment Defect Specimens

Name	Type	Material	Thickness	Percent Through-Wall	Angle from Vertical
44° Al	Calibration	Aluminum	50 mm	100%	-46°*
43° Al	Control	Aluminum	50 mm	100%	-47°
55° Al	Worst-Case	Aluminum	50 mm	100%	-35°
90° Corner	Calibration	Stainless Steel	15 mm	100%	0°
Defect Q	Worst-Case	Stainless Steel	15 mm	50%	+15°
Defect R	Control	Stainless Steel	15 mm	50%	0°

*Minus sign indicates that defect is angled away from the inspection probe.

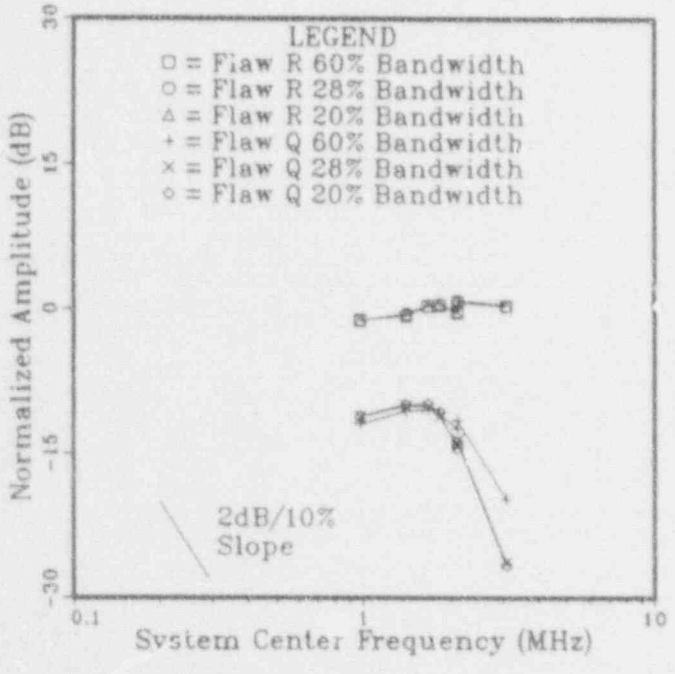

Figure 5.9. Center Frequency Sensitivity Measurement Results for 50% Through-Wall Defects

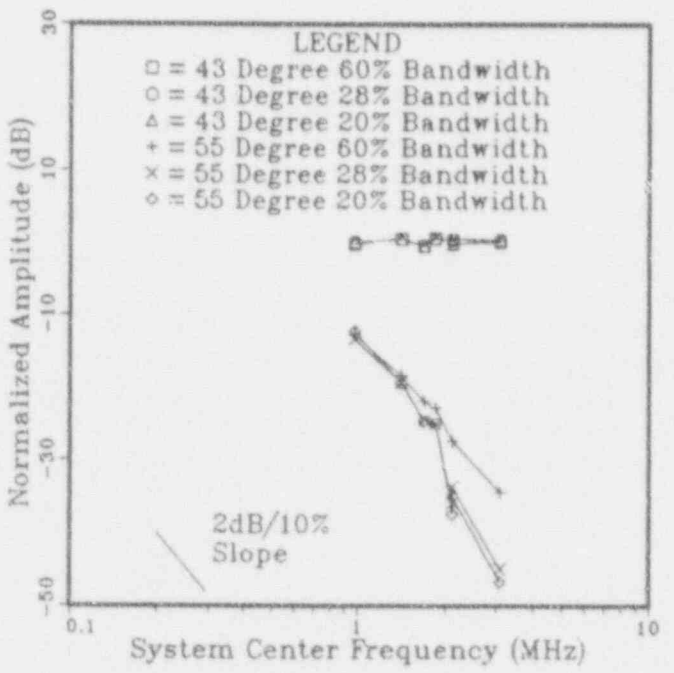

Figure 5.10. Center Frequency Sensitivity Measurement Results for Angle Blocks

6.0 Summary of Results

The model work was very effective in providing trending data to guide the empirical verification work. This methodology provided a more cost effective means to reach definitive conclusions concerning equipment operating tolerances. The detailed summary and conclusions reached in this study are:

- Model predictions were compared with data from multi-frequency experiments, and the validity of the model for predicting and calculating transfer functions for specular reflection from worst-case defects was established.

- The model was used to calculate postulated worst-case transfer functions for seven different combinations of transducer sizes, pipe wall thicknesses, and defect angles. The transfer functions were identified as worst case, because they displayed distinct minima at the equipment center frequency, and this feature produces sensitivity to changing frequency domain equipment parameters.

- An equipment bandwidth sensitivity study was performed using mathematical models for thin sections (piping) using postulated worst-case transfer functions. The results indicate that the ASME Code Section XI Appendix VIII bandwidth equipment tolerance of 10% is sufficient to ensure 2 dB signal amplitude repeatability.

- An equipment center frequency sensitivity study was conducted using mathematical models for thin sections employing several combinations of worst-case defects and equipment bandwidth. The model results indicate that none of the systems considered would be repeatable to within 2 dB after a center frequency change of 20%. The results suggest that a center frequency tolerance of ±10% is not sufficient for inspection systems with bandwidths less than 150%. A tolerance of ±5% appears appropriate for systems with bandwidths between 100% and 150%. A tolerance of 3.5% is indicated for systems with bandwidths between 20% and 100%. Systems with bandwidths less than 20% may be too sensitive to center frequency changes to permit repeatable inspection of worst-case defects.

- An experiment was performed to test the center frequency sensitivity of worst-case defect inspection. The experimental results were in general agreement with the modeling results, but the experimental results do not exhibit as much sensitivity to equipment center frequency changes as the modeling results. The experimental results indicate that a center frequency tolerance of ±5% is required for systems with bandwidths less than 30%, and a tolerance of ±10% is required for systems with bandwidths greater than 30%. A requirement of ±20% is not sufficient to guarantee inspection repeatability to within 2 dB for typical inspection systems. More work needs to be done to determine if the model is overly conservative in that it shows greater sensitivity than is found empirically.

- Calculations revealed that much of the frequency domain equipment parameter sensitivity was due to phase cancellation along the receiving transducer face. It is suggested that the receiving transducer for dual element search units and tandem configuration search units be made as small as possible to reduce sensitivity to equipment changes.

7.0 Future Work

The work documented in this report will be presented to be appropriate ASME Section XI Code bodies, and a specific recommendation will be made to reduce the tolerance to ±5% for the center frequency for bandwidths less than 30% and also to reduce the tolerance to ±10% for the center frequency for bandwidths greater than 30%.

The next step in the work reported in this paper will be to extend the ray tracing model to pressure vessels (thick sections). Several new capabilities are required:

- The ability to consider reflection from curved surfaces (e.g., nozzles) will be added to the model.
- The effects of grain scattering will be added to the model. This will probably be done by some type of frequency domain filtering of the data.
- The effects of cladding will be added to the model.

After the model is upgraded, worst-case defect acoustic systems will be identified for thick sections, and sensitivity studies will be performed as was done in the work reported here.

8.0 References

Adler, L., K. V. Cook, and W. A. Simpson. 1977. "Chapter 1: Ultrasonic Frequency Analysis," Research Techniques in Nondestructive Testing, Vol. 3, Academic Press Inc., Ltd., New York, pp. 1-49.

Bond, L. J. 1982. "Chapter 3: Methods for the Computer Modelling of Ultrasonic Waves in Solids", from Research Techniques in Nondestructive Testing, Vol. VI, R. S. Sharpe Editor, Academic Press, London, pp. 107-150.

Borloo, E., F. Lakestani, and F. Merli. 1988. PISC II - Parametric Study on the Effect of UT Equipment Characteristics (EEC) on Detection, Location, and Sizing, PISC III Report No. 10 - Final Report, available from Commission of the European Communities, Joint Research Center, Ispra, Italy.

Chapman, R. K. 1984. Ultrasonic Scattering from Smooth Flat Cracks: An Elastodynamic Kirchhoff Diffraction Theory (Main Report), CEGB Report NWR/SSD/84/0059/R PWR/RCC/MWG/P(84)378.

Coffey, J. M. and R. K. Chapman. 1983. "Application of Elastic Scattering Theory for Smooth Flat Cracks to the Quantitative Prediction of Ultrasonic Defect Detection and Sizing", Nuclear Engineering, Vol. 22, No. 5, October, pp. 319-323.

Coffey, J. M., R. K. Chapman, and D. J. Hanstock. 1982. The Ultrasonic Detectability of a Postulated "Worst Case" Flaw in a PWR Vessel, CEGB Report NWR/SSD/82/0045/R PWR/RCC/MWG/P (82)99.

Doctor, S. R., D. J. Bates, L. A. Charlot, H. D. Collins, M. S. Good, H. R. Hartzog, P. G. Heasler, G. A. Mart, F. A. Simonen, J. C. Spanner, and T. T. Taylor. 1986. Integration of Nondestructive Examination (NDE) Reliability and Fracture Mechanics, NUREG/CR-4469, PNL-5711, Vol. 1, pp. 6-17, U.S. Nuclear Regulatory Commission, Washington, D.C. 20555.

Doctor S. R., D. J. Bates, L. A. Charlot, M. S. Good, H. R. Hartzog, P. G. Heasler, G. A. Mart, F. A. Simonen, J. C. Spanner, A. S. Tabatabai, and T. T. Taylor. 1986. Nondestructive Examination (NDE) Reliability for Inservice Inspection of Light Water Reactors, NUREG/CR-4469, PNL-5711, Vol. 2, pp. 16-35, U.S. Nuclear Regulatory Commision, Washington, D.C. 20555.

Doctor, S. R., D. J. Bates, R. L. Bickford, L. A. Charlot, J. D. Deffenbaugh, M. S. Good, P. G. Heasler, G. A. Mart, F. A. Simonen, J. C. Spanner, A. S. Tabatabai, T. T. Taylor, and L. G. VanFleet. 1986. Nondestructive Examination (NDE) Reliability for Inservice Inspection of Light Water Reactors, NUREG/CR-4469, PNL-5711, Vol. 3, pp. 2-4, U.S. Nuclear Regulatory Commision, Washington, D.C. 20555.

Doctor, S. R., D. J. Bates, J. D. Deffenbaugh, M. S. Good, P. G. Heasler, G. A. Mart, F. A. Simonen, J. C. Spanner, T. T. Taylor, and L. G. VanFleet. 1987. Nondestructive Examination (NDE) Reliability for Inservice Inspection of Light Water Reactors, NUREG/CR-4469, PNL-5711, Vol. 4, pp. 4-6, U.S. Nuclear Regulatory Commision, Washington, D.C. 20555.

Doctor, S. R., J. D. Deffenbaugh, M. S. Good, E. R. Green, P. G. Heasler, G. A. Mart, F. A. Simonen, J. C. Spanner, T. T. Taylor, and L. G. VanFleet. 1987. Nondestructive Examination (NDE) Reliability for Inservice Inspection of Light Water Reactors, NUREG/CR-4469, PNL-5711, Vol. 6, pp. 30-39, U.S. Nuclear Regulatory Commision, Washington, D.C. 20555.

Doctor, S. R., J. D. Deffenbaugh, M. S. Good, E. R. Green, P. G. Heasler, G. A. Mart, F. A. Simonen, J. C. Spanner, and T. T. Taylor. 1988. Nondestructive Examination (NDE) Reliability for Inservice Inspection of Light Water Reactors, NUREG/CR-4469, PNL-5711, Vol. 7, pp. 37-52, U.S. Nuclear Regulatory Commision, Washington, D.C. 20555.

Doctor, S. R., J. D. Deffenbaugh, M. S. Good, E. R. Green, P. G. Heasler, F. A. Simonen, J. C. Spanner, and T. T. Taylor. 1989. Nondestructive Examination (NDE) Reliability for Inservice Inspection of Light Water Reactors, NUREG/CR-4469, PNL-5711, Vol. 8, pp. 2.21-2.34, U.S. Nuclear Regulatory Commision, Washington, D.C. 20555.

Doctor, S. R., J. D. Deffenbaugh, M. S. Good, E. R. Green, P. G. Heasler, F. A. Simonen, J. C. Spanner, and T. T. Taylor. 1989. Nondestructive Examination (NDE) Reliability for Inservice Inspection of Light Water Reactors, NUREG/CR-4469, PNL-5711, Vol. 9,

pp. 3-13 to 3-45, U.S. Nuclear Regulatory Commision, Washington, D.C. 20555.

Fitting, D. W. and L. Adler. 1981. Ultrasonic Spectral Analysis for Nondestructive Evaluation, Plenum Press, New York.

Good, M. S. and E. R. Green. 1989. "A Shear-Wave Microprobe Utilizing Surface-Wave Mode Conversion," Review of Progress in Quantitative Nondestructive Evaluation, Vol. 8A, Plenum Press, New York, New York, pp. 881-888.

Goodman, J. W. 1968. Introduction to Fourier Optics, McGraw-Hill, New York, New York.

Graff, K. F. 1975. Wave Motions in Elastic Solids, Ohio State University Press, pp. 311-343.

Green, E. R. 1989. "Worst-Case Defects Affecting Ultrasonic Inspection Reliability", Materials Evaluation, Vol. 47 No. 12, December 1989, pp. 1401-1407.

Green, E. R. 1990. "The Effect of Equipment Bandwidth and Center Frequency Changes on Ultrasonic Inspection Reliability: Modeling and Experimentation Results", to be published in Review of Progress in Quantitative Nondestructive Evaluation, Vol. 9, Plenum Press, New York, New York.

Green, E. R. and G. A. Mart. 1989. "Modeling Frequency Domain Effects for Ultrasonic Flaw Detection", Review of Progress in Quantitative Nondestructive Evaluation, Vol. 8B, Plenum Press, New York, New York, pp. 2259-2266.

Gregor, M. M. 1984. "The Influence of Probe and Instrument Data on Ultrasonic Testing Results", in Third European Conference on Nondestructive Testing, Florence, October 15-18, 1984, pp. 84-92.

Heyman, J. S. and J. H. Cantrell, Jr. 1977. "Application of an Ultrasonic Phase Insensitive Receiver to Material Measurements," in 1977 Ultrasonics Symposium Proceedings, IEEE Cat. No. 77CH1264-1SU, pp. 124-127.

Jungman, A., F. Cohen-Tenoudji, and G. Quentin. 1977. "Diffraction Experiments in Ultrasonic Spectroscopy; Preliminary Results on the Characterization of Periodic or Quasi-Periodic Surfaces," in Conference Proceedings of Ultrasonics International 1977, IPC Science and Technology Press, pp. 385-396.

Krautkramer, J. and H. Krautkramer. 1983. Ultrasonic Testing of Materials, Third Edition, Springer-Verlag, New York, New York.

Kuhn, G. J. and A. Lutsch. 1961. "Elastic Wave Mod. Conversion at a Solid - Solid Boundary with Transverse Slip." The Journal of the Acoustical Society of America, Vol. 33, No. 7, July 1961, pp. 949-954.

Langenberg, K. J. and V. Schmitz. 1986. "Numerical Modeling of Ultrasonic Scattering by Cracks," Nuclear Engineering and Design, 94, pp. 427-445.

MacDonald, D. E. and S. M. Walker. 1987. Effects of Ultrasonic Equipment Variations on Crack Length Measurements, EPRI NP-5485, available from Research Reports Center, P.O. Box 50490, Palo Alto, CA 94305.

Mart, G. A. and S. R. Doctor. 1987. "Modeling for Quantifying Ultrasonic Test System Component Interaction (The Interaction Matrix Study)", Proceedings of Eighth International Conference on Nondestructive Evaluation in the Nuclear Industry, Orlando, Florida (November 17-20, 1986), ASM International, pp. 325-331.

McElroy, J. T. 1977. "Detailed Analysis of the Fundamental Ultrasonic Response Data from Stainless Steel Stress Corrosion Crack Specimens," Project TPS 75-620, available from Southwest Research Institute, Quality Assurance Systems and Engineering Division, Post Office Drawer 28510, San Antonio, Texas.

Miller, G. F. and H. Pursey. 1954. "The Field and Radiation Impedance of Mechanical Radiators on the Free Surface of a Semi-Infinite Isotropic Solid," Proceedings of the Royal Society, pp. 521-541.

Murgatroyd, R. A., P. J. Highmore, S. F. Birch, T. Bann, and A. T. Ramsey. September 12, 1987. Flaw Characterization Using the Tandem and TOFD Techniques, Draft Final Report on EEC/UKAEA Contract No. 2871-85-12EN Isp GB. Risley Nuclear Laboratories, Harwell, United Kingdom.

Posakony, G. J. 1986. "Experimental Analysis of Ultrasonic Responses from Artificial Defects", Material Evaluation, 44, December, pp. 1567-1572.

Scruby, C. B., K. R. Jones, and L. Antoniazzi. 1986. Journal of Nondestructive Evaluation, Vol. 5, Nos. 3/4, pp. 145-156.

Silk, M. G. 1984 Ultrasonic Transducers for Nondestructive Testing, Adam Hilger Ltd, Bristol, United Kingdom.

Temple, J. A. G. 1985. Developments in Theoretical Modelling for Ultrasonic NDT, POST-SMIRT Seminar No. 2 - ISPRA 28/29 August 1985, Available from Theoretical Physics Division, AERE Harwell, Didcot, Oxon. OX11 0RA, United Kindgom.

DISTRIBUTION

No. of
Copies

OFFSITE

2 J. Muscara
NRC/RES
Mail Stop NS 217C

C. Z. Serpan
NRC/RES
Mail Stop NS 217C

F. P. Gillespie
NRC/NRR
Mail Stop 12 G18

M. R. Hum
NRC/NRR
Mail Stop 7 D4

G. Johnson
NRC/NRR
Mail Stop 7 D4

E. L. Murphy
NRC/NRR
Mail Stop 7 D4

J. E. Richardson
NRC/NRR
Mail Stop 7 D26

B. E. Thomas
NRC/NRR
Mail Stop 7 D4

W. S. Schwink
NRC/NRR
Mail Stop 7 D4

Branch Chief
NRC/NRR EMCB
Mail Stop 7 D4

No. of
Copies

J. P. Durr
NRC/Region I

E. H. Gray
NRC/Region I

M. C. Modes
NRC/Region I

J. T. Wiggins
NRC/Region I

J. J. Blake
NRC/Region II

A. R. Herdt
NRC/Region II

J. Shackelford
NRC/Region II

K. Ward
NRC/Region III

I. Barnes
NRC/Region IV

W. McNeill
NRC/Region IV

C. A. Clark
NRC/Region V

T. Gray
Center for NDE
Ames Laboratory
Iowa State University
Ames, IA 50010

D. S. Kupperman
Materials Science Center
Argonne National Laboratory
9700 S. Cass Avenue
Building 212
Argonne, IL 60439

R. B. Thompson
Center for NDE
Ames Laboratory
Iowa State University
Ames, IA 50010

B. P. Newberry
Mail Stop 70
Dept. of Aerospace Engrg.
University of Cincinnati
Cincinnati, OH 45221

FOREIGN

A. Rogerson
Building RD-9
NRL, AEA Technology
Risley Warrington WA3 6AT
Cheshire
United Kingdom

J. R. Tomlinson
NDT Application Centre
Nuclear Electric plc
Timpson Road
Wythenshawe
Manchester M23 9LL
United Kingdom

ONSITE

50 Pacific Northwest Laboratory

E. S. Andersen
R. E. Bowey
D. M. Boyd
S. H. Bush
A. A. Diaz
S. R. Doctor (28)
M. S. Good
B. F. Gore
M. S. Greenwood
R. V. Harris
P. G. Heasler
R. L. Hockey
R. J. Kurtz
F. A. Simonen
J. C. Spanner
T. T. Taylor
T. V. Vo
Publishing Coordination
Technical Report Files (5)

NRC FORM 335 (2-89) NRCM 1102, 3201, 3202

U.S. NUCLEAR REGULATORY COMMISSION

BIBLIOGRAPHIC DATA SHEET

(See instructions on the reverse)

1. REPORT NUMBER (Assigned by NRC, Add Vol., Supp., Rev., and Addendum Numbers, if any.)

NUREG/CR-5871
PNL-8064
Vol. 1

2. TITLE AND SUBTITLE

Development of Equipment Parameter Tolerances for the Ultrasonic Inspection of Steel Components

Application to Components Up to 3 Inches Thick

3. DATE REPORT PUBLISHED

MONTH: June YEAR: 1992

4. FIN OR GRANT NUMBER

FIN B2289

5. AUTHOR(S)

ER Green, SR Doctor, RL Hockey, AA Diaz

6. TYPE OF REPORT

Technical

7. PERIOD COVERED (Inclusive Dates)

8. PERFORMING ORGANIZATION – NAME AND ADDRESS (If NRC, provide Division, Office or Region, U.S. Nuclear Regulatory Commission, and mailing address; if contractor, provide name and mailing address.)

Pacific Northwest Laboratory
Richland, WA 99352

9. SPONSORING ORGANIZATION – NAME AND ADDRESS (If NRC, type "Same as above"; if contractor, provide NRC Division, Office or Region, U.S. Nuclear Regulatory Commission, and mailing address.)

Division of Engineering
Office of Nuclear Regulatory Research
U.S. Nuclear Regulatory Commission
Washington, DC 20555

10. SUPPLEMENTARY NOTES

11. ABSTRACT (200 words or less)

This report documents work performed at PNL on the effect of frequency domain equipment interactions on the reliability of ultrasonic inservice inspection. The primary focus of this work is to provide information to the NRC on the acceptability of equipment parameter tolerances as given in the ASME Boiler and Pressure Vessel Code Section XI Appendix VIII. Mathematical models were developed for the entire ultrasonic inspection system including sound propagation through the inspection sample. The models were used to determine worst-case inspection scenarios for thin sections (piping), and these worst-case inspection scenarios were then used in sensitivity studies to determine the suitability of equipment parameter tolerances. Ultrasonics literature was reviewed to find worst-case inspection scenarios outside the scope of the model used, but none that were significantly worse were found. Experiments were performed to confirm the important modeling results. The model predicted that ASME Code tolerances for equipment bandwidth are acceptable, but tolerances for center frequency are too broad to provide reliable inspection of worst-case defects using narrow band systems. Experiments confirmed the basic trends predicted by the model, but the model shows greater sensitivity than is found empirically.

12. KEY WORDS/DESCRIPTORS (List words or phrases that will assist researchers in locating the report.)

nondestructive evaluation, nondestructive testing, modeling of ultrasonic equipment, ultrasonic modeling of flaws, ultrasonic testing, ultrasonic equipment characterization, ASME Code

13. AVAILABILITY STATEMENT

Unlimited

14. SECURITY CLASSIFICATION

(This Page) Unclassified

(This Report) Unclassified

15. NUMBER OF PAGES

16. PRICE

UNITED STATES
NUCLEAR REGULATORY COMMISSION
WASHINGTON, D.C. 20555-0001

OFFICIAL BUSINESS
PENALTY FOR PRIVATE USE, $300

SPECIAL FOURTH-CLASS RATE
POSTAGE AND FEES PAID
USNRC
PERMIT NO. G-67

1 of 2

1 of 2